Setup for measuring the state of polarisation by means of nematic liquid crystals

by
Carlos Espona Torrent (Matr. Num. 1623292)

Bachelor's Thesis

for the bachelor of
Industrial Engineering

submitted at
Vienna University of Technology (TU Wien)

Supervisor
Ao.Univ.-Prof. Dipl.-Ing. Dr.techn. Gerhard Liedl

Institute for Production Engineering and Laser Technology

Faculty of Mechanical and Industrial Engineering

Vienna, June 2017

Abstract

An online monitoring and adaptive control during laser material processing is necessary for quality assessment and a relatively new way consists in using the information given by the inclination of the keyhole. In this project an existing electro-optical device is tested and improved in order to measure the polarisation state of the infrared light by means of nematic liquid crystals which is emitted by a thermal emitter that simulates a heated workpiece . The main improvement which has been carried out is the unification of various functions in one LabVIEW program with the goal of making a more compact setup and a fully automated process for the later transfer of the device onto a robot used for laser welding. Moreover a description about all the components of the device is given and also a checking of these has been performed. Finally some recommendations for further studies related to improving the LabVIEW program and enhancing the setup are given.

Keywords: laser material processing, quality assessment, online monitoring, inclination of the keyhole, polarisation of the light, nematic liquid crystals.

Acknowledgement

I would like to thank all the people who have helped me during the time that I have been performing this project. First of all my supervisor Prof. Gerhard Liedl who made me everything easier from the beginning, by offering many different topics for the project, to the end, by helping me with every doubt that I have had. Asst. Gerald Humenberger who has solved many problems that I have had everyday in the laboratory. My friends Ana, Luis and Carlos who have spent their time reading and revising all the Bachelor's Thesis.

Finally I would like to thank Pierre Drobniak who built the electro-optical device in his Master's Thesis that has been improved and tested for his selfless help when I needed it by making skype meetings or facebook chatting.

Contents

1 Introduction

1.1 Justification and motivation for the project

Nowadays laser based technologies have become strongly important or even dominant in material processing for industrial applications like welding, cutting, drilling, surface engineering, marking, coating, materials deposition, annealing and hardening [23]. Lasers have had such an incredible growth because of its intrinsic ability for continuous development and flexibility of use. As consequence industrial laser is considered a flexible machine tool because its light can be controlled accurately depending on the target and thus provides opportunities for innovation in material processing [33]. Therefore the research and the industrial use of lasers in material processing has not stopped increasing and it will also continue to challenge mainstream manufacturing processes as companies move to high precision manufacturing applications (Fig.1.1).

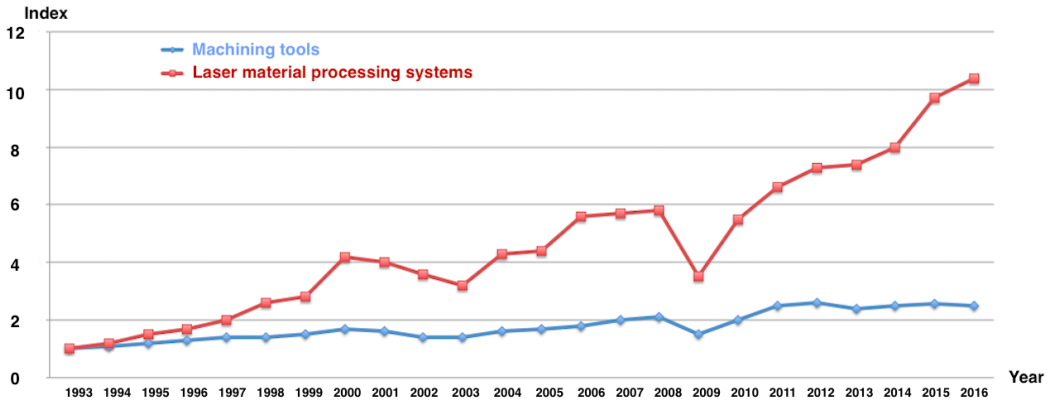

Figure 1.1: Global market for laser systems for materials processing and machine tools market in euro indexed to 1993 volume [1]

Also it has continued the lasers development in analysis, spectroscopy, metrology, communications and medical applications [43], however this project is focused in material processing. As it has already said lasers are used in many different applications but also treat with many different materials (metals and alloys, ceramics and glasses, polymers and composites), different modes of beam-material interaction (thermal and athermal) and it exists different types of laser machines depending on their active medium, wavelength, power, energy and mode of operation so possibilities offered by laser are endless [33].

A really important aspect during laser material processing is checking the quality of the

material which is being machined in real time in order to receive the necessary information and therefore being able to adjust parameters to improve the process. Checking the quality of the surface once the materials has been machined could give a very general information about the process telling if it has been right or not nevertheless it does not provide enough data to control the process properly . Thus an online monitoring and adaptive control during laser processing is necessary [23]. For it beam-material interactions produce characteristic emissions which contain information and that can be used [29].

Related to this quality assessment during the process different methods as the following exist. Using acoustic emission that at specific frequencies contains important diagnostic information [31], measuring the space charge voltage induced on an electrically insulated welding nozzle (which gives information about the welding performance) [39] or using high-speed optical and x-ray transmission methods [40]. The method that is going to be used in this project is about using the information given by the behavior of the keyhole. A relatively new way to analyze this keyhole consists in using the infrared radiation emitted by the heated laser machined surface.

During the process of laser welding the shape of the keyhole is a little bit inclined as it can be observed in Fig.1.2.

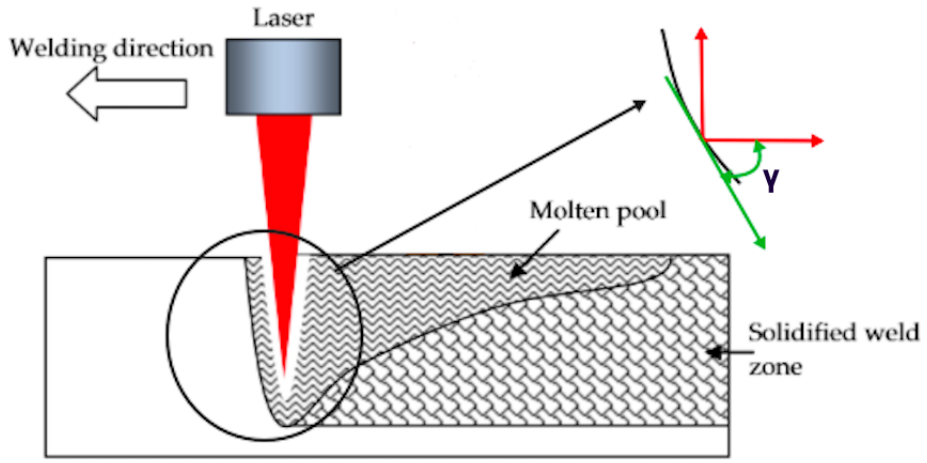

Figure 1.2: Inclined angle of the keyhole γ while laser welding [38]

The same phenomenom happens during the process of laser cutting where the shape of the cutting is inclined and during the process of laser drilling at the end of the hole. So the study of this is useful for many different laser processes, however focusing on this project one of the last and most difficult goals is to install an optical device for measuring polarisation and with it the inclination angle of keyhole γ specifically onto a robot used for laser welding.

Therefore to analyze the keyhole and with it make this quality assessment during the process is necessary to know the value of this inclined angle γ. So the sequence to compute it would be the following:

- Measuring the polarisation state of the light which depends on the measured angle.
- Calculating the angle of radiation of the emitted light by the heated body.
- Computing the inclined angle of the keyhole γ .

So this Bachelor's Thesis tries to get all the necessary information to compute this inclined angle focusing on the first step of the mentioned process and for it an existing electro-optical assembly is tested and improved.

1.2 Goals

The main goal of the Bachelor's Thesis is to test and improve an existing electro-optical device built in a Master's Thesis [28] which function is to measure the emission of an infrared radiating heated body by means of nematic liquid crystals. These measurements provide the necessary information to calculate the state of polarisation of a partially linear polarised infrared radiation and later would be able to provide a quality assesment during the process of laser processing by computing the angle of radiation and with it the inclined angle of the keyhole.

These tests and improvements consists of different tasks which are the following. At first installing the device in order to measure the polarisation of a fully linear polarised light emitted by a thermal emitter instead of a laser heated radiating surface. Secondly improving the configuration by unifying different functions in one LabVIEW program to control the measuring device which consists in making the whole computation fully automated. Afterwards the third main task would have been transfering the device onto a robot used for laser welding and finally testing it on the top of a laser processing head in order to compute the inclined angle. Unfortunately there has not been enough time to make it.

As this is a research project the objective is trying to advance as much as possible with the proposed problem in the available time. Therefore at the end of the project in Sec.6 and Sec.5 what has been achieved and what should be done in future is commented.

1.3 Similarities and distinctiveness with previous projects

This Bachelor's Thesis is the continuation of the investigation made in a previous Master's Thesis [28] which has tried something totally new, measuring the state of polarisation of an infrared light using nematic liquid crystals. This last aspect is what makes it new, the fact of using nematic liquid crystals in the Liquid Crystal Variable Retarder of the measuring device in order to make a quality assessment during the laser material

processing by computing the inclined angle. Other investigations [46] have used the emitted thermal radiation to get detailed information useful for monitoring and controlling quality in laser processes nevertheless it does not use nematic liquid crystals. The main objective of this project is the same as the one carried on the mentioned Master's Thesis so the optical device that has been used and the theory behind the computation is the same. The difference is in the way of performing some experiments and how the data are obtained and processed with the aim of improving the setup focusing on the electronics.

Regarding the quality assessment during the process other different methods have been commented in Sec.1.1. Another Thesis which aim is to measure the light polarisation using nematic liquid crystals is [24] but in this one the light consists in a HeNe laser, not in an IR-emitter or a heated surface.

So analyzing these previous investigations, all of them have many similarities about the used setup, goals or equipment, however none of them tries to do what is wanted to achieve in this thesis in the way that here is performed.

1.4 Methodology

This section aims to make a brief description to allow the reader to clearly understand how the project has been carried out by explaining its development over time, which elements have been used to obtain the data and how the experiments were performed.

1.4.1 Time management

The duration of this Bachelor's Thesis has been four months. During the first month a very general information about laser, laser welding and quality assessment was compiled by reading books about basics of laser technology. Later in the second month more specific information about measuring the polarisation of the light and using nematic liquid crystals like scientific articles was searched and the first sections of the project were started to be written. In the following month all the installation of the setup, the construction of the LabVIEW program and also the realization of the experiments was made while the writting of the report at the same time. Finally the last month this report was finished and checked to make the appropiate corrections.

1.4.2 Equipment and programs

In this section all the equipment and programs that have been used to make possible the electro-optical work are commented, nevertheless the device itself is not described here but it is done in Sec.3.

For the realization of the experiments the following devices have been used: an oscilloscope to make some simply measurements for the positioning of some components, a generator to provide the necessary voltage and current in order to generate the light

with the IR-emitter, a signal generator to check that the device works (instead of the LabVIEW program), an amplifier to amplify the signal measured by each photodiode, a computer to run the LabVIEW program in order to monitor the electro-optical device and a PCI NI 6024E [2] card (Fig.1.3a) with the NI-TBX 68 pin screw terminal [3] (Fig.1.3b) accessory to generate and measure the signals with the LabVIEW program. It is considered not necessary to explain exactly which model of each device that has been used because of with ordinary ones it is possible to get what is required, however some technical specifications about the PCI NI 6024E are important to know so these are included in the appendix in Sec.7.1.

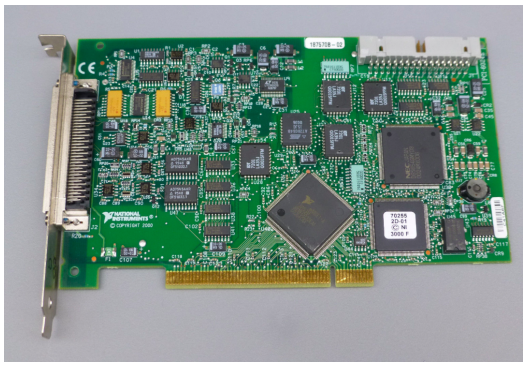

(a) PCI NI 6024E card to generate and simulate signals

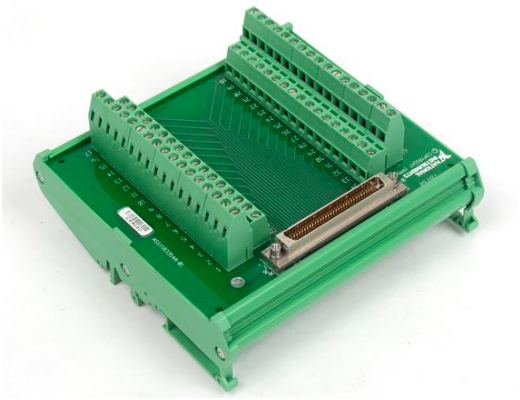

(b) NI-TBX 68 pin screw terminal

Figure 1.3: Card and pin screw terminal used to generate and measure signals using LabVIEW

Regarding the informatic programs that have been used these are: LabVIEW 2013 to make measurements and computation fully automated and Excel 2010 to approximate and get the function which fits with the behavior of the LCVR as it is explained in Sec.3.3.1.

1.4.3 Comments about the realization of experiments

Some remarks are considered important to take into account to facilitate the repetition of the experiments that have been carried out. It must be considered that in this Thesis the improved device has just measured fully linear polarised light, however it should be able to measure partially linear polarised light.

First of all the wavelength that has been measured during the whole thesis has been around 1500nm due to it was the one which better suited with all the components of the electro-optical device that were chosen. To make the assembly all the components were fixed using adapters and shafts and these were set in a rail which has an optical scale to measure distances. In order to know which polarisation state is being introduced by

the PSG polariser, a graduated circle has been used (Fig.1.4).

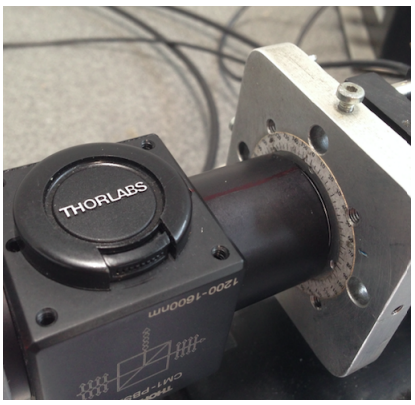

Figure 1.4: Graduate circle to set a polarisation state that is being generated

During all the experiments the electro-optical device was covered with a black piece of cardboard with the objective of avoiding the influence of the surroundings infrared light which variates depending on many different factors. Previously in [28] only the Beam Splitter was covered because of the adapter of photodiode 1 is transparent, however this has been improved by covering all the device.

For the computation the data that have been used is the main value of the measurements made by each photodiode due to each signal does not variates too much and then that can be accepted.

At first the experiments were tried to be carried out with another card, which is the NI 6009 [4], nevertheless it could not provide more that 5V so some alternatives were necessary. Two alternatives were thought: making an aditional LRC circuit to get the desired voltage or using another card which already was set in the computer. So the easiest solution was using the card NI PCI 6024E with the NI-TBX 68 pin screw terminal.

2 Theoretical background

2.1 Behavior of the keyhole and thermal radiation

2.1.1 Inclined angle of the keyhole

First of all, as the final objective is to install the optical device onto a robot for laser welding to compute the inclined angle of the keyhole it is essential to explain what laser welding consists in and which phenomenom is going to be studied. An illustrative picture of the laser welding process showing the geometry of the keyhole is given in Fig.2.1.

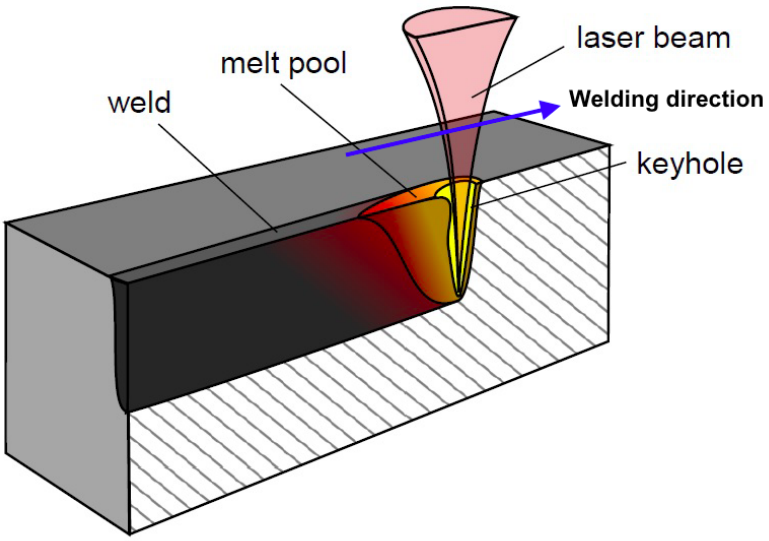

Figure 2.1: Sketch of the laser welding process [5]

Laser welding is an equilibrium between the heating and cooling within a spatially localized volume overlapping two or more solids in the way that a liquid pool is formed and remains stable until solidification [29]. This liquid melt pool is created by absorption of incident radiation, and depending on it and the uniform dissipation of heat inside the workpiece that balance is maintained. Some of the advantages in comparison to conventional welding techniques are proposed in [29] and the main pro is its ability to narrowly focus laser radiation to small area and as consequence be a strongly accurate technique. It is a joining technology with high quality, high precision, high performance, high speed, good flexibility and can be easliy automated [23]. A really interesting aspect of laser welding to be researched is the identification of those parameters which influence its stability and reproducibility and after it develop different ways to control these parameters. In this control of the process is where this project final goal is focused, to make

a quality assessment during the process of laser welding by measuring the polarisation of the emitted radiation of the heated workpiece in order to have information to calculate the inclined angle of the keyhole.

This inclined angle of the keyhole can provide many information about the process because of it is related to the welding speed, the absorbed laser intensity (related at the same time with the plume temperature and luminosity), penetration depth and incident laser power[23].

2.1.2 Thermal radiation

The emitted thermal radiation can provide a lot of information while monitoring and controlling quality about temperature distribution and geometrical structures [46]. Thermal radiation is electromagnetic radiation and as consequence it is commented in the following sections however before it is necessary to explain what p- and s- polarisation concept is and what a black body is in order to relate it with the real radiation emitted by a heated surface and make possible the computation of the angle of radiation and with it the inclined angle of the keyhole as it has been shown in the explained process in Sec.1.1.

First of all the polarisation of an incident light beam and the reflected one can be divided in two perpendicular components to make the study of it easier [28]. These two components are p- polarisation and s- polarisation. P- polarisation component is perpendicular to the direction of propagation and contained in the plane of incidence while s- polarisation is perpendicular to the direction of propagation and parallel to the reflecting surface as it is shown in Fig.2.2.

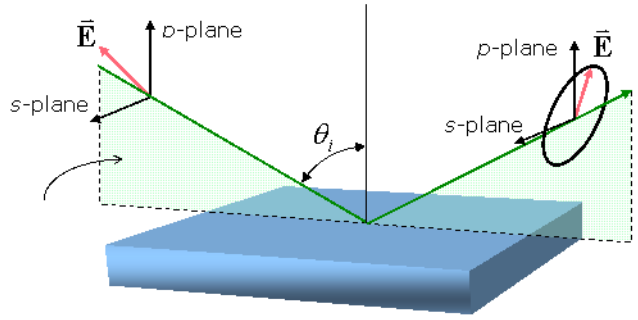

Figure 2.2: P- and s- polarisation components of an incident and reflected light beam [6]

Secondly a black body emmits blackbody radiation which is equal to the full amount specified by Planck's law and it has a specific spectrum and intensity which depends only on the body's temperature. It is a theoretically ideal radiator and abosrber of energy at all electromagnetic wavelengths and it can be approximated by a hollow insulated enclosure containing a small hole in one wall where the incident energy goes inside and gets reflected again and again against the inner wall (Fig.2.3).

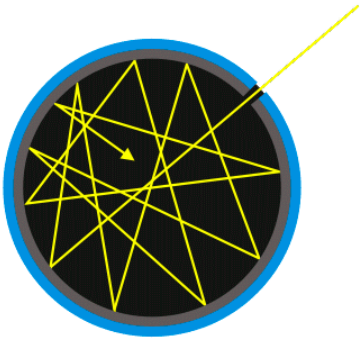

Figure 2.3: Representation of a conceptual Black Body [7]

Planck's law describes the spectral density of that radiation at a given temperature [34]. No physical body can emit as higher thermal radiation as the emitted by a black body [42], nevertheless it is really useful because of it exists relation between the radiation density of a real surface and a black body which can be expressed by the spectral emissivity $\boldsymbol{\epsilon}$ parameter [46]. This emissivity $\boldsymbol{\epsilon}$ parameter depends on many different factors which are wavelength, temperature, surface conditions and material. More over this parameter can relate angle of radiation and state of polarisation (p- and s- polarisation). As it is proved in [46] the ratio $\frac{\epsilon(\text{s-polarised})}{\epsilon(\text{p-polarised})}$ depends on the angle of radiation β and therefore this angle can be obtained by computing this ratio. Once this angle of radiation is known, the inclination angle of the keyhole could be computed [46].

2.2 Basics of optics

For this section, most of the equations and developed theory have been extracted from the book [26], which is perfectly in accordance with the mathematical description that is necessary in relation to the polarisation of light. Moreover all the mathematical description made in this project consists in a short summary of the deep theoretical research made in [28].

2.2.1 Basics of the light and degree of polarisation

Light has a dual nature as it is demonstrated in [27]. It behaves sometimes as a particle and sometimes as a wave. A really important concept is the wavelength which is used to classify electromagnetic waves in different types of radiation and focusing in the one which is the center of attention in this project, infrared radiation (IR) is between 700nm and 1000000nm. Talking about polarisation of the light it is convenient to represent it as a wave, however light should not be forgotten as a particle because this behavior is really important in laser technology. Considering the light as an electromagnetic wave its behavior can be described with the following Fig.2.4.

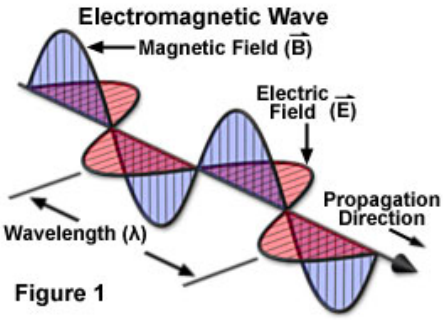

Figure 2.4: Description of the propagation of the light [8]

As it can be observed in Fig.2.4 the light is composed of an electric field and a magnetic field which oscillate perpendicularly to the direction of propagation. Nevertheless talking about polarisation the magnetic field is insignificant in comparison with the electric so it is neglected in optical measurement [26]. Polarisation speficies the geometrical orientations of the oscillations of the electric field by telling the direction or plane. There are three types of polarisation of the light: linear, circular and eliptic [44] which are well shown in Fig.2.5.

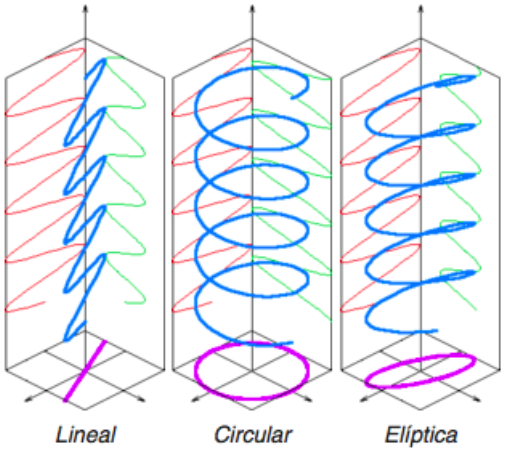

Figure 2.5: Three types of polarisation of the light

Is it is really important to take into account that light is a combination of polarised and unpolarised light, so the electric field consists in the addition of both and as consequence the full intensity of the light beam I can be described as (Eq.2.1):

$$I = I_{up} + I_p \tag{2.1}$$

where I_{up} is the intensity of the unpolarised component and I_p the intensity of the polarised component.

Regarding this combination of both parts a really important parameter which is the degree of polarisation DoP appears (Eq.2.2) [26]:

$$DoP = \frac{I_p}{I_{up} + I_p} \tag{2.2}$$

So the degree of polarisation DoP describes quantitetively the polarisation of the light. The extreme values are 0 for a fully unpolarised light beam and 1 for a perfectly polarised one.

2.2.2 Stoke parameters

Stoke parameters are the components of the Stokes vector $\vec{S}$ (Eq.2.3) which describes polarisation of an electromagnetic radiation in the intensity domain and come from the study of the electric field. It carries complete information on the intensity and state of polarisation and they may be normalized by dividing each parameter by S_0 [44].

$$\vec{S} = \begin{pmatrix} S_0 \\ S_1 \\ S_2 \\ S_3 \end{pmatrix} \tag{2.3}$$

For linear polarised light the last Stoke parameter S_3 is equal to 0 and therefore in these cases a simplified vector of three components should be used. Different examples of Stokes vectors for different polarization states can be consulted in many sources as [44].

The degree of polarisation DoP can be written depending on these Stokes parameters (Eq.2.4) :

$$DoP = \frac{I_p}{I_{up} + I_p} = \frac{(S_1^2 + S_2^2 + S_3^2)^{\frac{1}{2}}}{S_0} \tag{2.4}$$

where S_0 is the sum of I_{up} and I_p as it can be observed.

2.2.3 Mueller matrices

The physical process that a partially polarised light beam suffers when it crosses an optical device can be described with the Mueller matrix A of the device. It allows the computation of the output Stokes vector $\vec{S_{out}}$ considering an input Stokes vector $\vec{S_{in}}$ which is altered by the optical device [44]. Therefore this is the resulting Eq.2.5 [32]:

$$\vec{S_{out}} = A \times \vec{S_{in}} \tag{2.5}$$

where $A = \begin{pmatrix} a_{11} & a_{12} & a_{13} & a_{14} \\ a_{21} & a_{22} & a_{23} & a_{24} \\ a_{31} & a_{32} & a_{33} & a_{34} \\ a_{41} & a_{42} & a_{43} & a_{44} \end{pmatrix}$, $\vec{S_{out}} = \begin{pmatrix} S_{out,0} \\ S_{out,1} \\ S_{out,2} \\ S_{out,4} \end{pmatrix}$ and $\vec{S_{in}} = \begin{pmatrix} S_{in,0} \\ S_{in,1} \\ S_{in,2} \\ S_{in,4} \end{pmatrix}$.

Mueller matrices allow the study of the process that a light beam suffers among an optical assembly with many optical components by multiplying their Mueller matrices. It is really important to take into account the order in the multiplication which depends on the order in which the light beam meets the components. The first component with Mueller matrix A_1 that the light beam meets multiplies the input Stokes vector $\vec{S_{in}}$ and then the Mueller matrix of the next component A_2 multiplies on the left of the previous component, and so on as it can be observed in Eq.2.6:

$$\vec{S_{out}} = A_2 \times A_1 \times \vec{S_{in}} \tag{2.6}$$

In [36] some examples of Mueller matrices for different optical components are given so later when the Mueller matrix of a component would be necessary it would be extracted from this source.

As it will be explained later in Sec.3.1 it is essential to understand what a linear polariser (analyser) and a variable retarder (LCVR) make in order to make the mathematical description of the device in Sec.3.2. A linear polariser changes a non linear light beam into a linear one and to measure the polarisation of the emergent linear polarised light beam is necessary to define the plane of polarisation which is made with the angle between the polariser and a fixed reference. A variable retarder provides a variable phase shift and its behavior is explained in Sec.2.4.

2.3 Calculation of an unknown linear Stokes Vector

The goal of this section is to show how to compute an incident unkown partially linear polarised Stokes vector for a known Mueller matrix of an optical assembly by making some measurements of the emergent light beam. Therefore the objective is the determination of this partially linear polarised Stokes vector $\vec{S_{in}}$ (Eq.2.7):

$$\vec{S_{in}} = \begin{pmatrix} S_{in,0} \\ S_{in,1} \\ S_{in,2} \\ 0 \end{pmatrix} \tag{2.7}$$

The Mueller matrix M (Eq.2.8) of the optical assembly is known and depends on the applied voltage.

$$M(V) = \begin{pmatrix} a_{11}(V) & a_{12}(V) & a_{13}(V) & a_{14}(V) \\ a_{21}(V) & a_{22}(V) & a_{23}(V) & a_{24}(V) \\ a_{31}(V) & a_{32}(V) & a_{33}(V) & a_{34}(V) \\ a_{41}(V) & a_{42}(V) & a_{43}(V) & a_{44}(V) \end{pmatrix} \tag{2.8}$$

Once the incident light beam has passed through the whole optical assembly the Stokes vector is $\vec{S_{out}}$ and using Eq.2.5 the following system is achieved (Eq.2.9):

$$\vec{S_{out}} = \begin{pmatrix} S_{out,0} \\ S_{out,1} \\ S_{out,2} \\ S_{out,3} \end{pmatrix} = M \times \vec{S_{in}} = \begin{pmatrix} a_{11}(V)S_{in,0} + a_{12}(V)S_{in,1} + a_{13}(V)S_{in,2} \\ a_{21}(V)S_{in,0} + a_{22}(V)S_{in,1} + a_{23}(V)S_{in,2} \\ a_{31}(V)S_{in,0} + a_{32}(V)S_{in,1} + a_{33}(V)S_{in,2} \\ a_{41}(V)S_{in,0} + a_{42}(V)S_{in,1} + a_{43}(V)S_{in,2} \end{pmatrix} \tag{2.9}$$

However from the output light beam the only component of the Stokes vector $\vec{S_{out}}$ that can be measured is $S_{out,0}$ and so the Eq.2.10 is the one useful which is extracted from the system (Eq.2.9):

$$S_{out,0} = a_{11}(V)S_{in,0} + a_{12}(V)S_{in,1} + a_{13}(V)S_{in,2} \tag{2.10}$$

The values $a_{1j}(V)$ $(j = 1, 2, 3)$ and $S_{out,0}$ are known so there are three unknowns: $S_{in,0}$, $S_{in,1}$ and $S_{in,2}$. Nevertheless $S_{in,0}$ which is the full intensity of the incident light beam can be measured and as consequence there are only two unknowns and so only two equations (Eq.2.11) are required, what means it is necessary to take only measurements for two different voltages (V_1 and V_2).

$$\begin{aligned} S_{out,0}(V_1) &= a_{11}(V_1)S_{in,0} + a_{12}(V_1)S_{in,1} + a_{13}(V_1)S_{in,2} \\ S_{out,0}(V_2) &= a_{11}(V_2)S_{in,0} + a_{12}(V_2)S_{in,1} + a_{13}(V_2)S_{in,2} \end{aligned} \tag{2.11}$$

This equations can be rewritten in matrix form as (Eq.2.12):

$$\vec{J}(V_1, V_2) = B(V_1, V_2) \times \begin{pmatrix} S_{in,1} \\ S_{in,2} \end{pmatrix} \tag{2.12}$$

where $B(V_1, V_2) = \begin{pmatrix} a_{12}(V_1) & a_{13}(V_1) \\ a_{12}(V_2) & a_{13}(V_2) \end{pmatrix}$ and $\vec{J}(V_1, V_2) = \begin{pmatrix} S_{out,0}(V_1) - a_{11}(V_1)S_{in,0} \\ S_{out,0}(V_2) - a_{11}(V_2)S_{in,0} \end{pmatrix}$

Then in order to calculate $S_{in,1}$ and $S_{in,2}$ the used equation is Eq.2.13:

$$\begin{pmatrix} S_{in,1} \\ S_{in,2} \end{pmatrix} = B^{-1} \times \vec{J}(V_1, V_2) \tag{2.13}$$

To be able to use this equation (2.13) it is necessary that B is invertible and this is the case with the optical assembly used in this project as it is proved in [28]. Therefore carrying out the indicated computation it is possible to derive the state of polarisation by taking measurements for two different voltages. Nontheless it must be considered that other ways to make this computation are possible, this explanation is just the one which has been chosen and which better fits with the given conditions.

2.4 Basics of nematic liquid crystals

First of all it is really important to know what a liquid crystal is. This is an intermediate phase in symmetry and structure which has features from both the solid crystalline and the amorphus liquid state. They flow like liquids but at the same time they have ordering properties of solids [30]. Due to their dual nature (anisotropic physical properties of solids and rheological behavior of liquids) and their easy response to externally applied electric, magnetic, optical and surface fields liquid crystals have an incredible potential for scientific and technological applications [45].

There are different types of phases in which liquid crystals can appear and are called mesophases: nematic, cholesteric, smectic and ferroelectric [35]. Nevertheless nematic phase is the most interesant for electro-optical applications. Nematic liquid crystals molecules are still able to move around in the fluid (molecules have no orderly position and are free to move), however their orientation remains the same (all molecules are alligned approximately parallel to each other, they tend to point the same direction)[30] as it is shown in Fig.2.6.

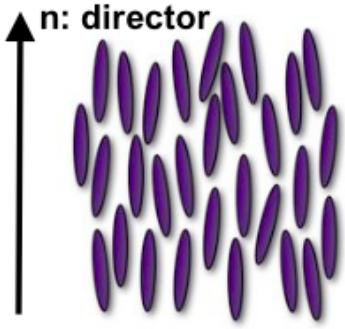

Figure 2.6: Molecules orientation and order in Nematic Liquid Crystals [9]

As consequence of the commented properties of nematic liquid crystals the polarisation of a light beam which passes through them can be altered. These are electrically variable waveplates (the absence of moving parts allows really high switching time around milliseconds) which alterate the retardance by applying a variable, low voltage waveform. It consists of a transparent cell filled with a solution of liquid crystal (LC) molecules and a voltage can be applied across the cell due to two parallel faces of the cell wall are coated with transparent conductive film [10] as it can be observed in Fig. 2.7:

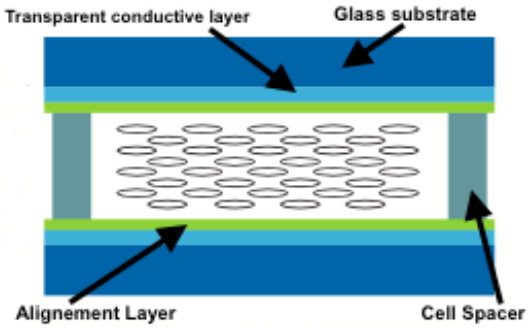

Figure 2.7: Scheme of a liquid crystals cell [10]

So a liquid crystal retarder allows to control the phase and with it the polarisation state of the transmitted light depending on the applied voltage which influence in the orientation of the molecules introducing a phase shift between the two components of the incoming polarised light beam as it can be observed in Fig. 2.8:

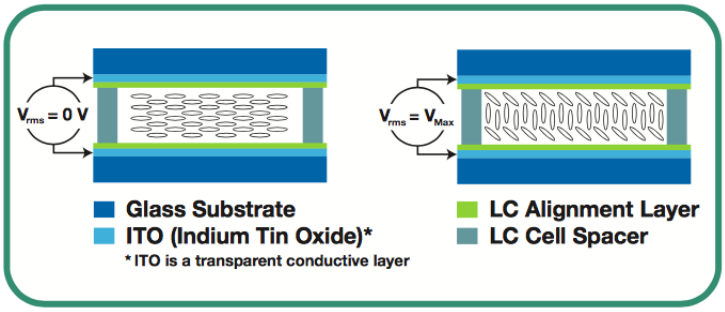

Figure 2.8: Rotation of the LC molecules when an electric field is applied between the two confining surfaces [10]

Regarding mathematics this component can be described with its Mueller matrix as it has already been said in Sec.2.2.3. Before it is really important to consider that the medium is birefringent so two axis of refraction must be used: slow-axis and fast-axis. Therefore the phase shift introduced depends on the relative orientation between the incident light beam polarisation vector and the slow-axis and fast-axis of the liquid crystal variable retarder [28]. Then the Mueller matrix of a liquid crystal variable retarder R can be written as (Eq.2.14)[25]:

$$R = \begin{pmatrix} 1 & 0 & 0 & 0 \\ 0 & C^2 + S^2\cos(\delta(V)) & SC(1-\cos(\delta(V))) & -S\sin(\delta(V)) \\ 0 & SC(1-\cos(\delta(V))) & C^2 + S^2\cos(\delta(V)) & C\sin(\delta(V)) \\ 0 & S\sin(\delta(V)) & -C\sin(\delta(V)) & \cos(\delta(V)) \end{pmatrix} \tag{2.14}$$

where α is the fast-axis azimuthal angle, δ is the phase shift, $C = \cos(2\alpha)$, $S = \sin(2\alpha)$ and V is the RMS voltage applied between the electrodes.

3 Description of the electro-optical device

3.1 Description of the structure and components

The optical device used in this project was developed and built in the aforementioned Master's Thesis [28]. Nevertheless a brief description about all the different parts and components, why were these chosen and which are their functions is considered essential. More detailed information and an approximation of the budget for the assembly can be found in [28] (which is around 2000 €). An important point to highlight is that this device is totally electrically controlled, without any moving or rotating part. As consequence of the fact that the device was disassembled, each component has been analyzed and photographed and then mounted appropiately for the realization of each experiment. A picture of the electro-optical device is given in Fig.3.1.

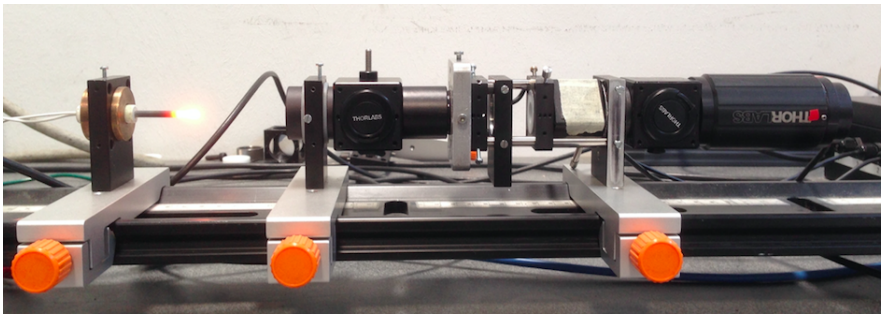

Figure 3.1: Electro-optical device

This device can be divided in two important parts: a simulator of the linear polarisation for the experiments which is the polarisation state generator (PSG) and an analyser of this generated linear polarisation which is the polarisation state analyser (PSA).

The PSG is made up of the following components:

- Infrared emitter (IR-emitter)
- Polariser (Polarising Beam Splitter)

While the PSA is made up of:

- Lens
- Filter
- Liquid Crystal Variable Retarder (LCVR)

- Non-polarising Beam Splitter (BS)
- Analyser (Polarising Beam Splitter)
- 2 Photodiodes

Observing Fig.3.2 can be understood more easily the structure of the device.

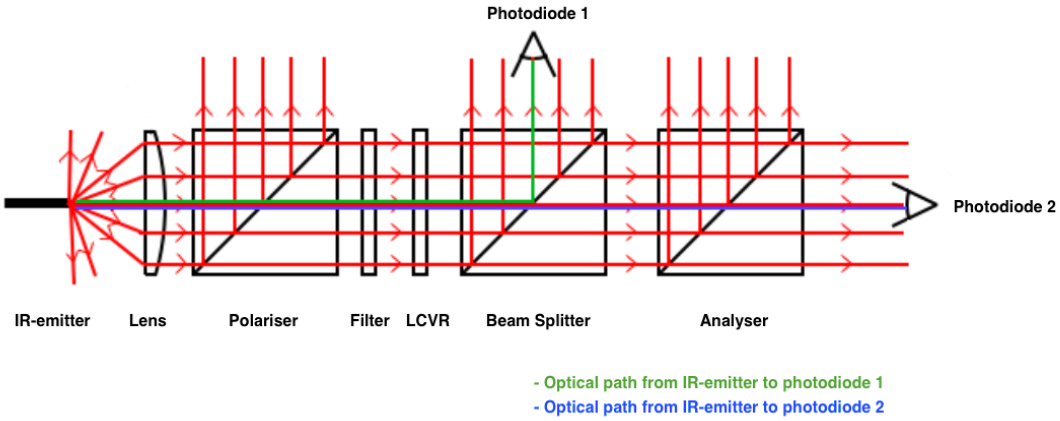

Figure 3.2: Structure of the electro-optical device

3.1.1 Infrared emitter

The aim of the IR-emitter (IR-Si295, Hawk Eye Technologies [11]) as its name indicates is being the infrared light source and therefore it simulates the infrared radiating heated surface emission which is being laser processed. The data given by Hawk Eye Techologies relating wavelength and emission starts only in 2000nm, nontheless it emits light around 1500nm which is the wavelength that has been used in the project.

A picture of this component is shown in Fig.3.3.

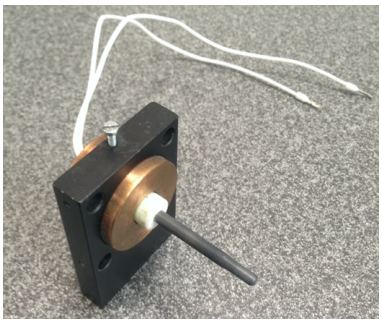

Figure 3.3: Infrared emitter IR-Si295

The IR-emitter must be controlled in order to generate the light. In Fig.3.4 it can be observed which intensity and voltage must be chosen.

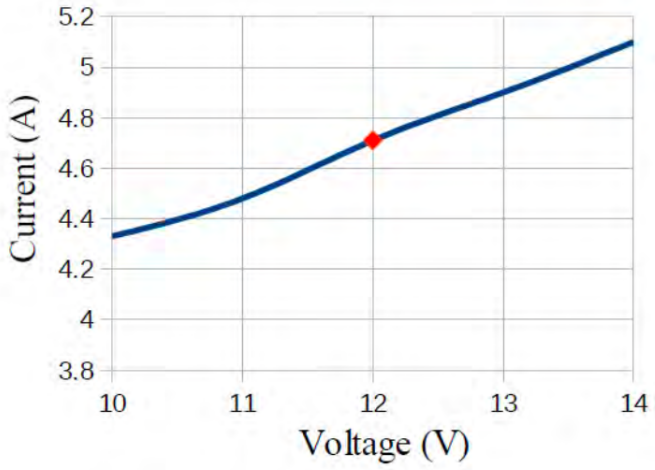

Figure 3.4: Current and voltage that should be chosen to monitor the IR-emitter [28]

To get this voltage and current that must be provided a powerful generator is used. This part of the monitoring has not been included in the unified LabVIEW program because if the device would be transfered onto a robot for laser welding the PSG would be removed and the radiation emitted by a heated body would be analyzed with the PSA.

3.1.2 Lens

The lens (LA4306, Thorlabs Inc [12]) is the first component of the device after the infrared emitter. Its target is to focus the emitted light from the tip of the IR-emitter in order to get a parallel light beam after the lens and therefore the intensity of the light after the lens should be approximately constant along the optical path. To get this parallel beam it is necessary to place the lens at a distance from the tip of the IR-emitter equal to the focal length of the lens for the used wavelength. Due to the fact that the information given by manufacturer is valid between 250nm and 400nm the focal length for 1500nm is unknown, so the obtaining of this focal distance is made in the first experiment in Sec.4.1 where it is concluded that for 1500nm of wavelength the focal distance is about 69mm.

This lens is strongly important due to an infrared radiating heated surface which is being laser processed emits light in all directions. And then this parallel beam is really necessary because of with it the difference between the intensity measured by each photodiode depends only on the components along each optical path which allows the calculation of the state of polarisation. In case that it would not be parallel it would be really difficult to know which part of this difference comes from the influence of the

components and which comes from the beam divergence. As it is possible to observe the optical path length of each photodiode in Fig.3.2 is different (for technical reasons related to the existance of the beam splitter) and if it would have been the same the beam divergence would not have influenced in measurements, however it has not been possible.

A picture of this component is presented in Fig.3.5.

Figure 3.5: LA4306 lens

The dimensions of the lens can be consulted at the end in appendix in Sec.7.2.

3.1.3 Polariser

The second part of the PSG is the polariser, but for technical reasons a polarising beam-splitter (CCMM1-PBS254/M, Thorlabs Inc [13]) with a 50:50 splitting behavior has been used which is shown in Fig.3.6.

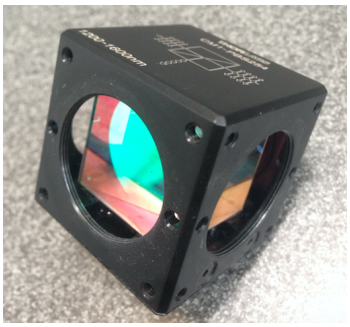

Figure 3.6: Polarising beam-splitter (CCMM1-PBS254/M)

After this component a linear polarised light beam is achieved, nevertheless because of only one of the outputs is used a loss of 50% occurs. The splitting behaviour of the component is shown in appendix in Sec.7.3 where it is possible to observe that for a P-polarised light as input, the output light has the same orientation angle with the same P-polarisation and with a transmission coefficient of approximately 100% for the used wavelength (around 1500nm).

3.1.4 Filter

Once the linear polarised light beam is achieved there is a filter (bk-1500-090-B bandpass filter, Interferonzoptik Elektronik GmbH [14]). Its target is to remove the stray light in order to filter the light beam because of the photodiodes are not only sensitive for 1500nm. Here it is a picture of this component in Fig.3.7.

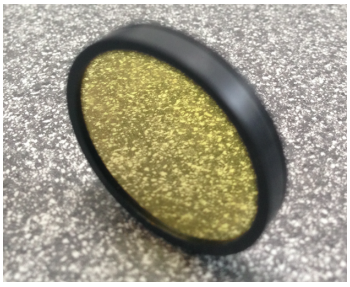

Figure 3.7: bk-1500-090-B bandpass filter

The spectrum after the filter reaches a peak for 1550nm with a 80% transmission coefficient (Interferenz Optik datasheet) and it is around 1470nm and 1550nm with a 70% transmission coefficient (relation between transmission coefficient and wavelength can be observed in the appendix in Sec7.4).

3.1.5 Liquid Crystal Variable Retarder(LCVR)

The next component of the optical device is the LCVR (LCC1111-C, Thorlabs Inc [15]) which aim is to alter the retardance by applying a variable square-wave voltage (a more detailed description about the LCVR controlling is given in Sec.3.3.1).

A picture of this component is given in Fig.3.8.

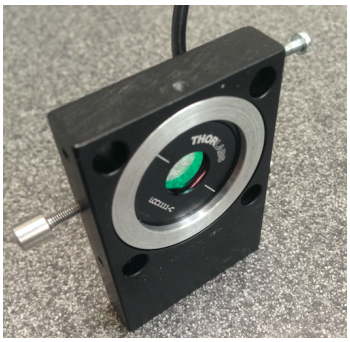

Figure 3.8: LCC1111-C LCVR

As it has been said it changes the retardance depending on the applied RMS voltage (Root Mean Square value) and this behavior is shown in Fig. 3.9.

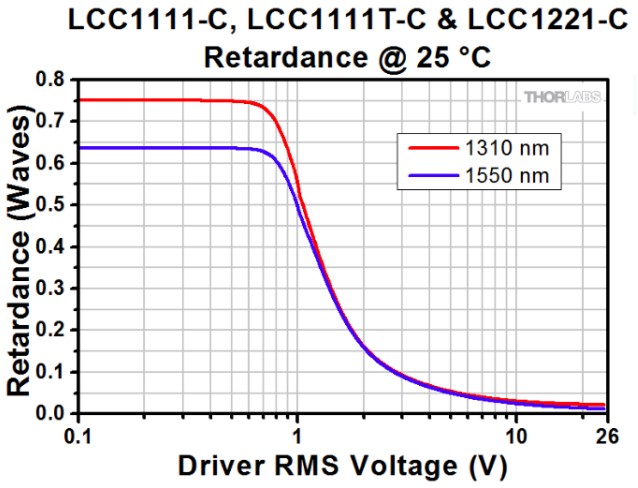

Figure 3.9: Relation between the phase shift induced between the slow-axis and fast-axis and the RMS voltage for 25°C [16]

This LCVR can be considered suitable for this project because of the transmission coefficient for around 1500nm wavelength is approximately 95% [15]. Further specifications can be consulted in [16].

Therefore by varying the RMS applied voltage it is possible to change the phase shift and the Mueller matrix of the Polarisation State Analyser (described in Sec.3.2).

3.1.6 Non-polarising Beam-splitter (BS)

After the disturbance produced by the LCVR in the linear polarised light beam there is a non-polarising beam-splitter (CCM5-BS018/M, Thorlabs Inc [17]) which is shown in Fig.3.10.

Figure 3.10: CCM5-BS018/M non-polarising beam-splitter [17]

This component works with a ratio of 50:50 approximately however this ratio depends on the polarisation state of the input light and therefore could change (according to Thorlabs technicians the splitting-ratio can vary by up to 10%). As it is possible to

observe in Fig.3.2 with it the measurement made by photodiode 1 in one output is possible and in the other output the light is directed towards the second photodiode passing through the analyser before.

3.1.7 Analyser

Before photodiode 2 the last component that the linear polarised light beam meets is the analyser which for technical reasons is a polarising beam-splitter, the same as the one presented previously in Sec.3.1.4. Here its goal is making possible the analysis of the state of polarisation of the incoming light by giving information about the linear part of it.

3.1.8 Photodiodes

The photodiodes are really important components in this assembly because of they are the ones which give the necessary information in order to compute the state of polarisation of the infrared radiation. Here it is a picture of the photodiode (G12180-010A, Hamamatsu) that has been used in both cases in Fig.3.11.

Figure 3.11: Photodiode G12180-010A Hamamatsu [18]

Regarding precision this photodiode has a photosensitive area of 1mm [19] and after the lens the light beam is about 25.4mm diameter therefore the sensitive surface is covered by the beam and then it can be considered an enough components alignement precision.

The goal of each photodiode is the following:

- Photodiode 1: it measures the intensity of the light before the analyser. This intensity of the incident light can be derived taking into account that it is after the LCVR and it has a 95% transmission coefficient.
- Photodiode 2: it measures the intensity of the light once it has been altered by the analyser. It is important to know that there is a loss due to the divergence of the light beam between the non-polarising beam-splitter (changes in the ratio of the BS and the analyser transmission) and the second photodiode.

The signals measured by photodiodes are very low (around hundreds of mV) so they must be amplified and for it the amplifier shown in Fig.3.12 is used. It must be plugged into the main electric current, then the two photodiodes must be connected to two of

the inputs and the corresponding outputs must be at the same level of amplification. This amplifier was developed in [41] and for further information it can be consulted.

Figure 3.12: Picture of the amplifier

3.2 Mathematical description

In this section the electro-optical device is described from a mathematical point of view by its Mueller matrix. All the following affirmations and calculations were made in [28] and this is a brief description about it, so for a more detailed one the cited thesis can be consulted.

First of all it should be clear that the data measured by photodiode 1 does not need more matrix computation because it almost gives the intensity of the incident light beam. On the other hand the calculation of the Mueller matrix of the path for photodiode 2 must be done. This matrix is a combination of a LCVR with an anlayser and then it can be written as (Eq.3.1):

$$M = \begin{pmatrix} 1 & 0 & 0 & 0 \\ 0 & C^2 + S^2\cos(\delta(V)) & SC(1-\cos(\delta(V))) & -S\sin(\delta(V)) \\ 0 & SC(1-\cos(\delta(V))) & C^2 + S^2\cos(\delta(V)) & C\sin(\delta(V)) \\ 0 & S\sin(\delta(V)) & -C\sin(\delta(V)) & \cos(\delta(V)) \end{pmatrix} \tag{3.1}$$

In this case as it been seen it is better to work with the 2×2 matrix B (Eq.3.2).

$$B = k \begin{pmatrix} C^2 + S^2\cos(\delta(V_1)) & SC(1-\cos(\delta(V_1))) \\ C^2 + S^2\cos(\delta(V_2)) & SC(1-\cos(\delta(V_2))) \end{pmatrix} \tag{3.2}$$

So this matrix B is proved in [28] as invertible by computing its determinant. Therefore analyzing the determinant attention must be paid that the phase shift introduced by the LCVR for V_1 is not the opposite of the phase shift introduced for V_2. As it can be observed matrix B depends on the voltage.

Finally the LCVR azimuthal angle θ must be defined which is really important for the device efficency and it should be 27.37° heeding [47]. It will be used a azimuthal

angle θ of 22.5°(angle between the fast axis of the LCVR and the horizon) because the LCVR bracket has a central circle with four holes which indicates angles of 45°, 135°, -135° and -45° to the horizon and then it is easy to set the LCVR to the specified angle of 22.5°.

3.3 Unified LabVIEW program

An unified LabVIEW program has been developed in order to improve the monitoring of the process. With this improvement a more compact measurement of the polarisation of an infrared radiation is achieved due to it can do at the same time in one program various functions that were made before with different devices and programs. It is considered useful to explain each function of the program comparing it to the one which existed before, to show how all the parts have been put together in order to access in one funtion or other, how is the interface with the user and how some improvements of the program have been carried out.

These functions are: signal generation (Sec.3.3.1), signal measurement (Sec.3.3.2) and computation (Sec.3.3.3) and are deeply explained in the following sections.

3.3.1 Signal generation

The goal of the part of the program which generates a signal is monitoring the LCVR and information about it is given by the manufacturer [20]. It must be controlled with a squared wave of 2kHz with an amplitude that can be varied from 0V to 25V of RMS (Root Mean Square) value. This wave must be without offset and therefore the RMS value is the same as the positive peak value. As it has already commented the phase shift that is provided by LCVR depends on this RMS value as it shown in Fig.3.9. This dependence is really important because for the experiments for each RMS value, the phase shift must be calculated in the LabView program for the computation of the state of polarisation. As two measurements with two different values of the squared signal are required this signal is proposed by the manufacturer (Fig.3.13):

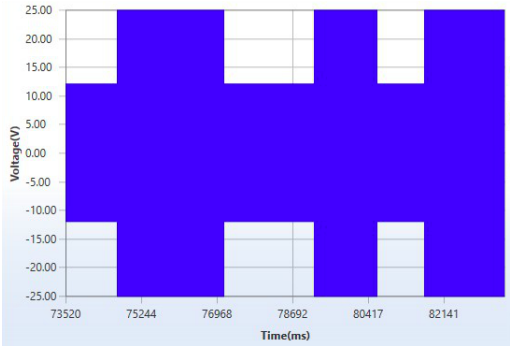

Figure 3.13: Plot of the squared signal that must be introduced in the LCVR [20]

Analyzing the proposed waveform by the manufacturer the way that has been achieved in this project is similar but not exactly the same. What has been done consists in generating a squared signal during the time that the user wants with a desired RMS value theoretically between 0 and 25 V, but for limitations of the NI PCI-6024 card it must be between 0 and 10V which is enough. So with this part a squared signal of 2kHz, without offset and with a desired RMS value is generated and the computation of the corresponding retardance is achieved. A picture of the block diagram part of the program which makes this function is in Fig.3.14:

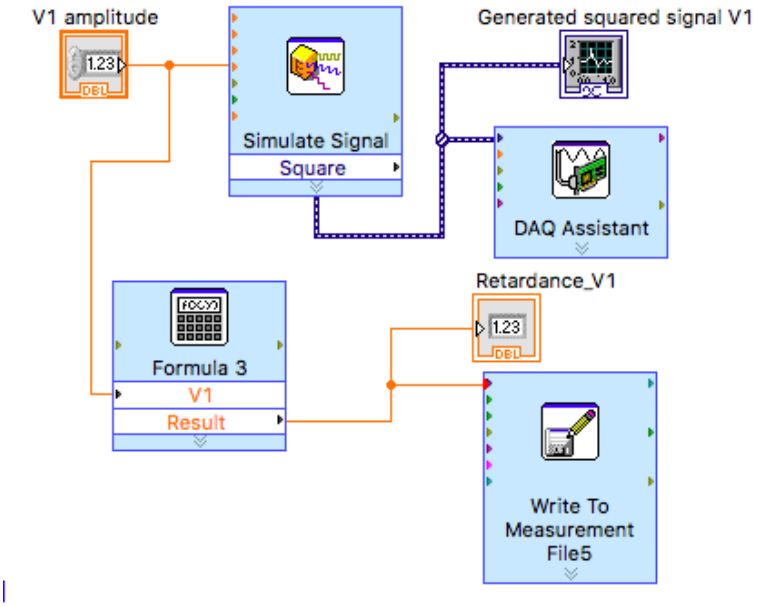

Figure 3.14: Block diagram of the LabVIEW program part which generates the desired squared signal

The block diagram consists in first of all a RMS value which must be introduced by the user and then the signal is simulated and sent to one card analog output which generates it. In the bottom of the diagram depending on the RMS value the appropiate retardance is computed and saved in a .LVM file which is read later in the part of the program described in Sec.3.3.3.

To get that formula which fits with the graph given by the manufacturer, Excel has been used by introducing some values of it and approximating it with a polynomial function of degree six. Other alternatives were considered like using a potential approximation which is also good but not that much and a logarithm approximation which is even worse. It must be considered that it has been approximated between 1V and 10V so the values that should be introduced by the user should be between both values or even better between 1V and 8V because for 9V or 10V the approximation is worse. Here this approximation is presented showing how it fits correclty and the formula in Fig.3.15:

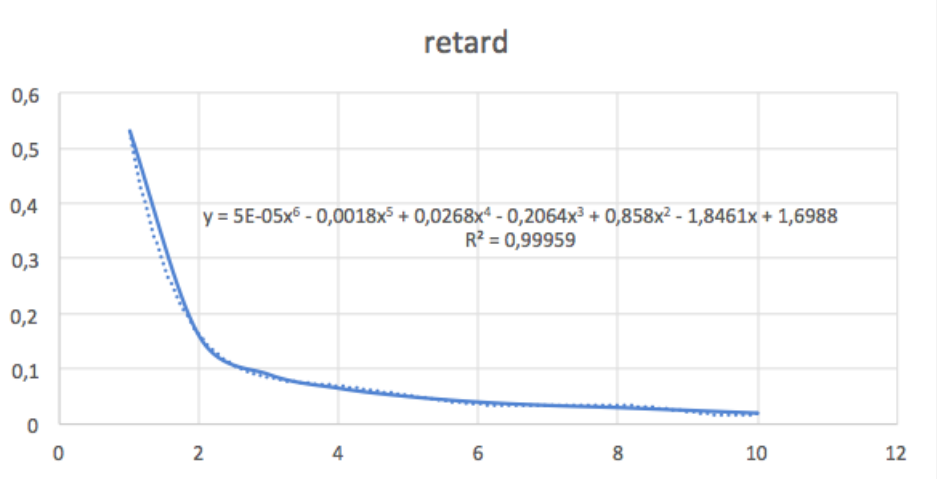

Figure 3.15: Approximation of the retardance curve depending on the RMS value between 1V and 10V

It can be observed in Fig.3.14 that this block diagram is for one RMS value and as consequence for one measurement, so this block diagram is duplicate in order to get the second measurement with another RMS value. When the user wants as it is explained in Sec.3.3.4 and Sec.3.3.5 the program proceeds to make the second measurement and then a second voltage can be applied.

Before in [28] this signal generation was achieved with a signal generator what implies the use of more equipment and more manipulation by the user to get this signal and also the obtaining of the retardance depending on the RMS value was done by the user observing the graph given by the manufacturer and as consequence more time was necessary.

3.3.2 Signal measurement

Signals received by photodiodes 1 and 2 are measured using the following acquisition program (Fig.3.16) which gets the mean value of each one and save these two values as .LVM file which later are read in Sec.3.3.3 in order to make the necessary computation. The acquired signal by each photodiode does not variate much over time so it can be averaged and this is the reason why the mean value is computed.

The block diagram consists at first in that two card analog inputs measure the signal of both photodiodes and for it, the user can choose the rate and number of samples (however it is considered that these vaules should not be changed and both are 1000 samples with a rate of 1000Hz). Then both signal data are written in an array of two columns and later each column is obtained in order to represent them separetely and to calculate the mean value of each signal.

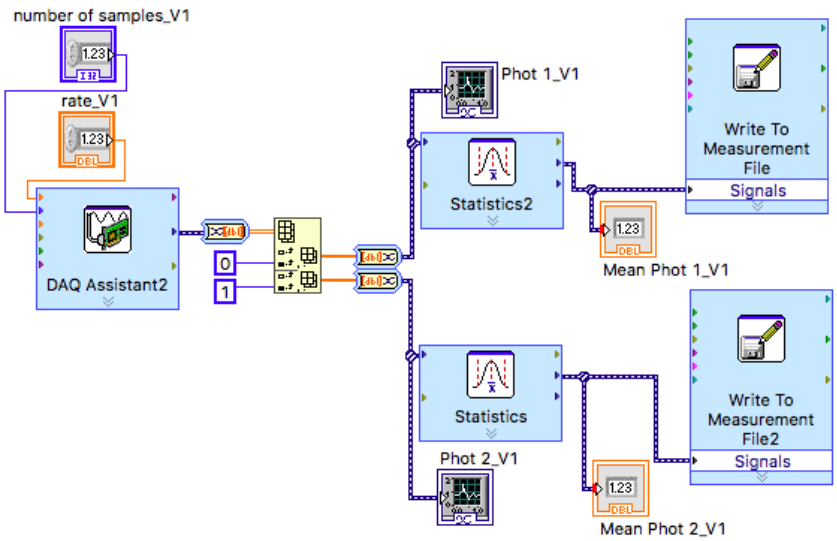

Figure 3.16: Block diagram of the LabVIEW program part which measures the signals of both photodiodes and saves the mean value in a .LVM file

The advantage obtained is that the mean value is achieved in the LabVIEW program without the need of another program as Excel, which was used in the previous version of the signal measurement LabVIEW program in [28] by saving the data in .TDMS files and later getting the mean value in Excel so the process to get these mean values was much longer.

3.3.3 Computation

The aim of this part consists in computing the azimuthal angle of the linear polarisation and the corresponding Stokes vector using the theory developed in Sec.2.3, specifically it consists in applying Eq.2.13 and getting matrix B as it is indicated in Eq.3.2. To make this computation it is necessary to read the values that the entire program has been saving which are the full intensity of photodiode 1, intensity measured by photodiode 2 for V_1, intensitiy measured by photodiode 2 for V_2, retardance for V_1 and retardance for V_2. This computation made with LabVIEW is shown in Fig.3.17.

This Fig.3.17 is hard to understand however it is not as complex as is looks, it just consists in simple calculations with matrices and vectors. This computation was made before with a Matlab program in [28] shown in Fig.3.18. By reading this code it is easier to know how the computation has been carried out in this project which is exactly the same but instead of using Matlab code, it has been performed with blocks using Lab-

VIEW. For a deeper explanation about what each line of the program is [28] can be consulted, nevertheless it just consists in solving the Eq.2.13.

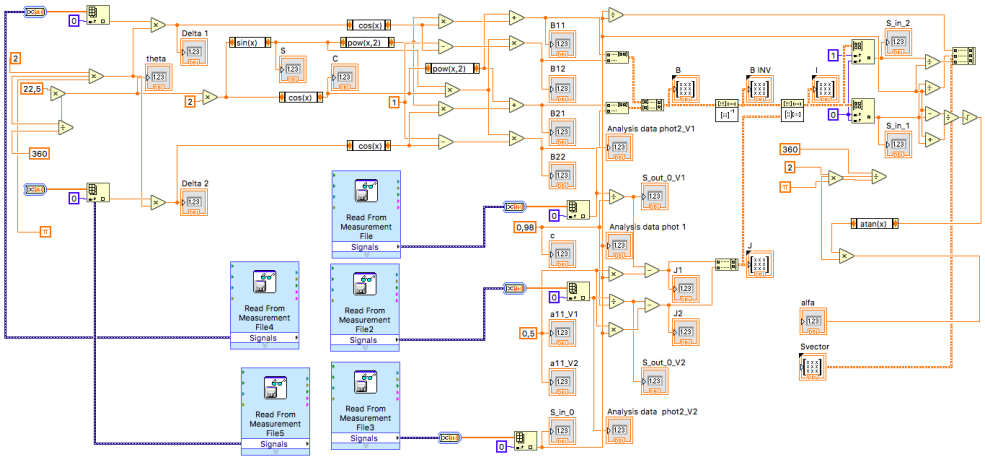

Figure 3.17: Block diagram of the LabVIEW program part which reads the data saved before and makes the whole computation of the azimuthal angle of linear polarisation and the Sokes vector

Maybe it is harder to implement this program with LabVIEW nevertheless once it is done it really makes the process much faster and more compact than if a Matlab program is used, what means that the data must be sent to Excel and then read by Matlab and computed.

One consideration must be done, in case that the device would be transfered onto a robot for laser welding this part of the program should include the computation of the angle of radiation and the inclined angle of the keyhole γ.

```
clear all; close all; clc;

% This program computes the value of the linear polarised incident Stokes
% vector as well as the azimuth angle of the linear polarisation.
% It requires the full intensity (photodiode 1) and the intensity of
% photodiode 2 for two different voltages on the LCVR.

% Definition of some constants
theta=(22.5/360)*2*pi;  % Angle between fast-axis of LCVR and horizon
C=cos(2*theta);         % Constant for simplification of matrix B
S=sin(2*theta);         % Constant for simplification of matrix B

%Transmission coefficient of the Analyser
c=0.98;

% Choice of the phase-shift introduced by the LCVR (in radian) for the 2
% different voltages
delta_1=0.53*2*pi;  %RMS=1V
delta_2=0.16*2*pi;  %RMS=2V

% Creation of the Matrix B
B=0.5*[ C^(2)+S^(2)*cos(delta_1) S*C*(1-cos(delta_1));
        C^(2)+S^(2)*cos(delta_2) S*C*(1-cos(delta_2))];

% Definition of values required to build vector J
S_out_0_V1=1.31/c;  % Intensity measured by photodiode 2 for delta_1
S_out_0_V2=0.92/c;  % Intensity measured by photodiode 2 for delta_2
a11_V1=0.5;         % Coefficient (1,1) of matrix A(V1)
a11_V2=0.5;         % Coefficient (1,1) of matrix A(V2)
S_in_0=1.34;        % Full intensity measured by photodiode 1

% Build-up of vector J
J=[S_out_0_V1-a11_V1*S_in_0;
   S_out_0_V2-a11_V2*S_in_0];

% Computation of the incident state of polarisation
I=inv(B)*J;         % I contains the second and third values of the
                    % incident Stokes vector.
S_in_1=I(1);
S_in_2=I(2);
S=[S_in_0;
   S_in_1;
   S_in_2]/S_in_0   % Build-up and normalisation of the incident Stokes
                    % vector S

% Computation of the azimuth angle of the linear polarisation
alpha=atan(sqrt((S_in_0-S_in_1)/(S_in_0+S_in_1)))*360/(2*pi)
```

Figure 3.18: Matlab program for the determination of the state of polarisation developed in [28]

3.3.4 Entire program

Once every part of the program has been understood it is really important to explain how everything has been conected in order to achieve the goals for which the program has been created.

The idea is the following: at first in the first step the squared signal with amplitude V_1 must be applied, the corresponding retardance must be approximated and saved as a .LVM file, the acquisition of the signals measured by both photodiodes for V_1 must be done and the mean value of these measurements must be computed and saved as a .LVM file. Secondly in the second step the same as what has been commented in the first step must be done but for V_2. Finally in the third step the program must read the values that have been saved before in the two previous steps, which are: full intensity of photodiode 1 (mean value measured by photodiode 1 for V_1 or V_2 because of it should be the same), mean value of the intensity measured by photodiode 2 for V_1, mean value of the intensity measured by photodiode 2 for V_2, retardance for V_1 and retardance for V_2. Once these values are read, the computation explained before must be done and the azimuthal angle of polarisation and the Stokes vector are obtained.

This idea has been carried out with the Case structure. The case selector is a numeric control which the user manipulates, when it is 0 the first step is performed, when it is 1 the second step is performed and when it is 2 the third one is performed. It can be easily understood how this case structure works in this program with the following scheme given in Fig.3.19.

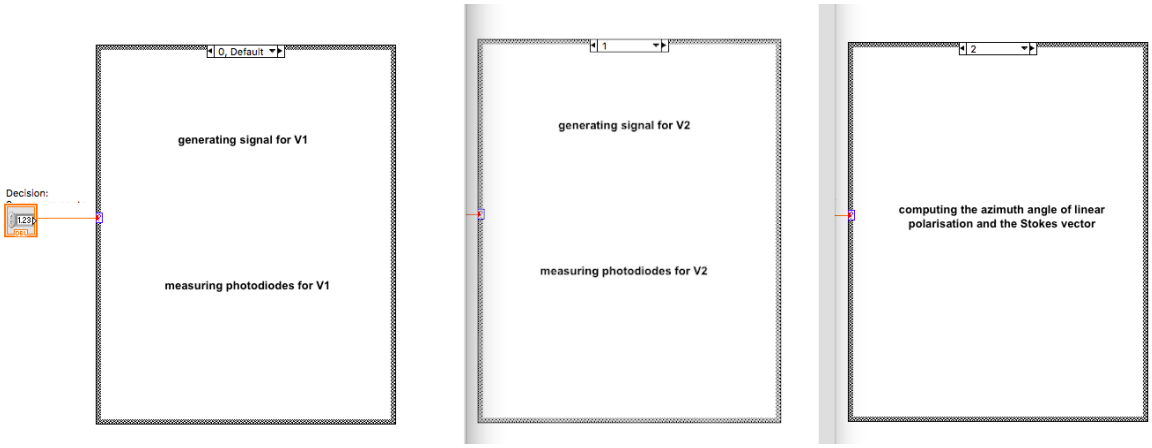

Figure 3.19: Scheme of how the case structure works in the LabVIEW program

So the block diagram of the entire program consists in that case structure with the decision numeric control and inside each case the three commented functions. The front pannel of this entire program is the following shown in Fig.3.20 in which all the computed values and matrices, generated signals and acquired signals in oscilloscopes can be observed.

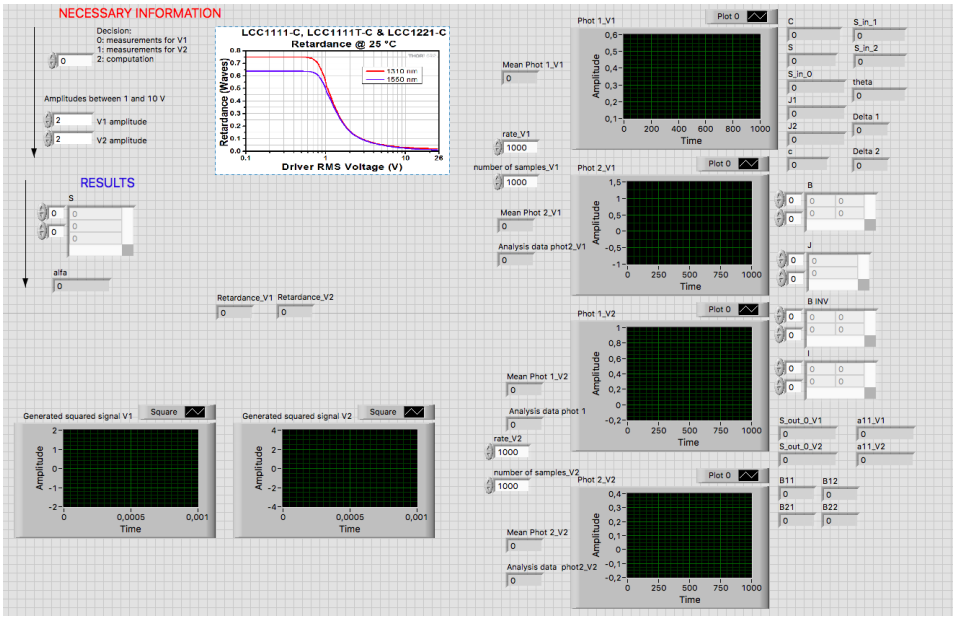

Figure 3.20: Front pannel of the unfied LabVIEW program

Another way to reach the objective which was thought consists in using a time sequence structure, that would have done each step depending on the time. Nontheless finally the one that has been explained was carried out because with the case structure the user can decide if a measurement must be repeated before going to the next step or not. This possible alternative is commented later in Sec.5.1.

3.3.5 Interface

Regarding what the user must do in order to use the LabVIEW program consists in the following. The front pannel should be opened and attention should be paid in this space shown in Fig.3.21.

Taking into account what has been expalined in the previous section before running the program the user should at first choose which pair of voltages wants to apply in the LCVR by introducing it it in V_1 amplitude and V_2 amplitude numeric controls. Also the user should set a 0 in the decision numeric control because it must be the first process. Then once the program is running the user should wait one second (or more) with the decision 0, then change it to 1 and wait one second (or more) and finally change it to 2 so then the azimuthal angle of polarisation and the Stokes vector are computed getting what was desired.

As it can be observed in Fig.3.21 there is a graph which is just put in order to show the user which is the retardance introduced in the LCVR depending on the chosen RMS voltage.

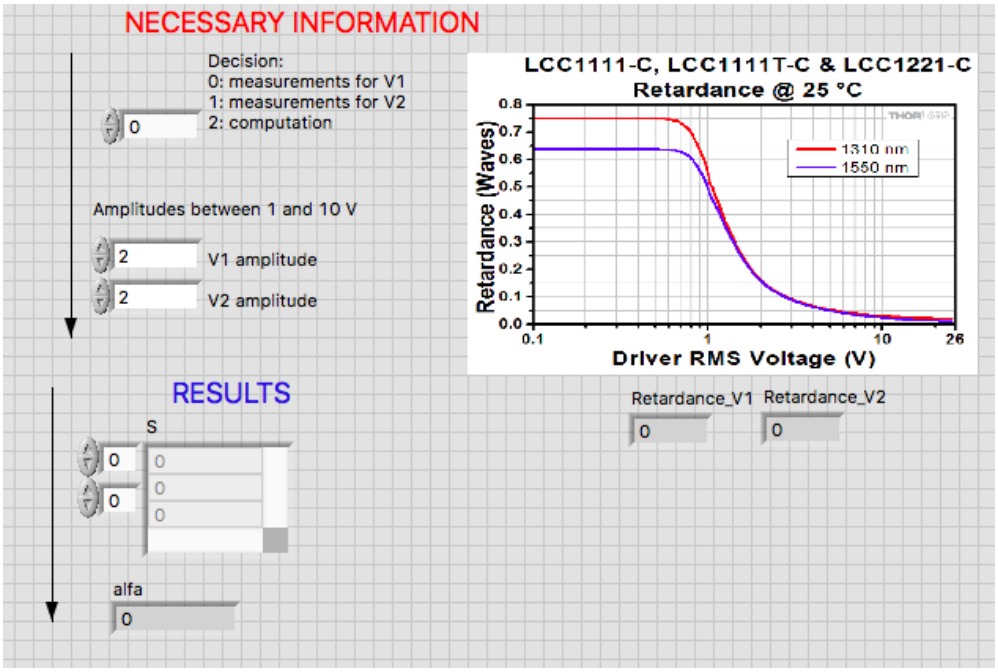

Figure 3.21: Part of the front pannel in which the user should focus on

Therefore with this unified LabVIEW program a more efficient and compact process has been achieved, saving equipment, time and manipulation made by the user. Some possible improvements of the interface and the program for further studies are commented in Sec.5.1.

3.3.6 Improvements

The objective of this section is explaining how some improvements must be carried out in order to have a fully automated process. In this process the user should just introduce the values of the two voltages at the beginning and press a button which starts to run the program. The difference is about that now the user does not need to change the decision numeric control to decide when the program gets into each case, now it is made automatically. To achieve this improvement the decision to get in each case consists in a chronometer. So when the user press the buttom then it starts to count, when it is zero before the user press it and the first second, it is performing the case 0, then when it is counting it goes into the case 1 when the chronometer is 1 and the same for 2. Finally the user press again the button to set the chronometer in zero and make possible the performance of new measurements.

To achieve this way of running the program, the decision would be now the chronometer and it must show just seconds (it just need to have the precision of units). The structure of this chronometer is shown in Fig.3.22:

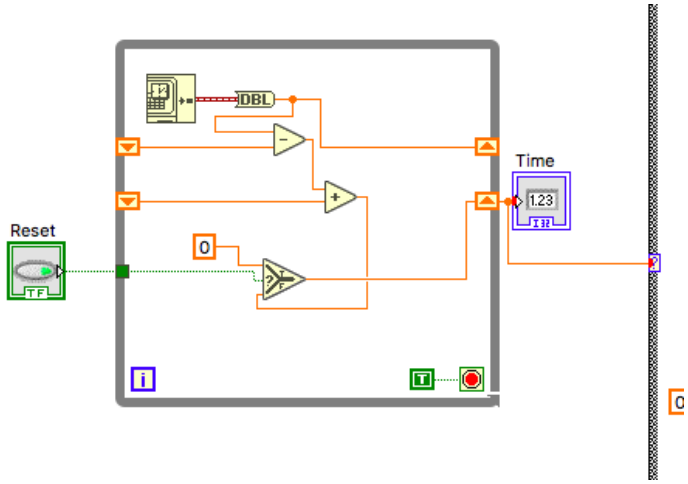

Figure 3.22: Block diagram of the decision with the chronometer

Then the interface would be the following presented in Fig.3.23:

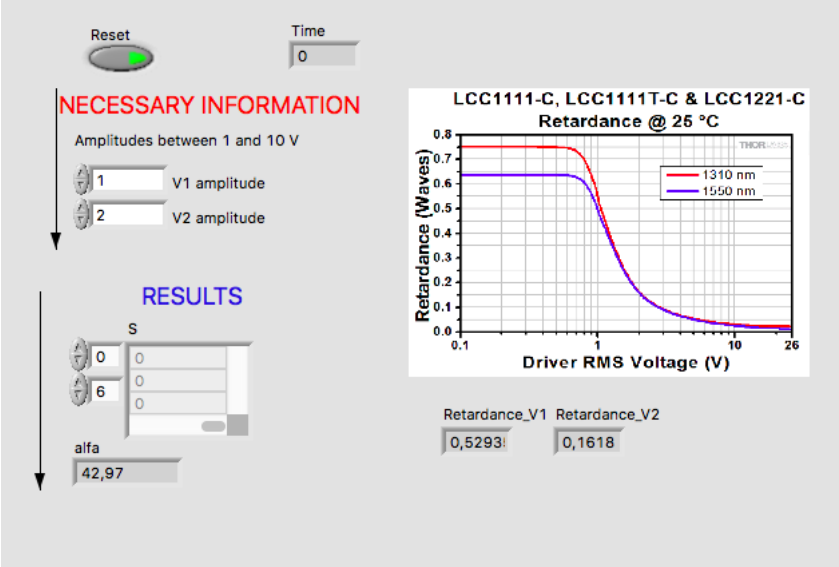

Figure 3.23: Front pannel of the fully automated program

4 Experiments and discussion of the results

4.1 Determination of the lens focal length

For the measurements to compute the state of polarisation first of all it is essential to have the lens in the appropriate distance from the IR-emitter. This focal length is not given by the manufacturer for 1550nm of wavelength and this is the cause that makes necessary this experiment.

The goal consists in positioning the lens at distance of its focal length from the IR-emitter tip in order to make that the light focuses on a paralell beam after the lens because of at first the IR-emitter emits light in all directions. Then after the lens the measured voltage by a photodiode should be the same regardless of the distance that the photodiode is. The configuration of the device for this experiment is shown in Fig.4.1 in which the polarising beam-splitter, the LCVR and the analyser are not necessary so these are removed.

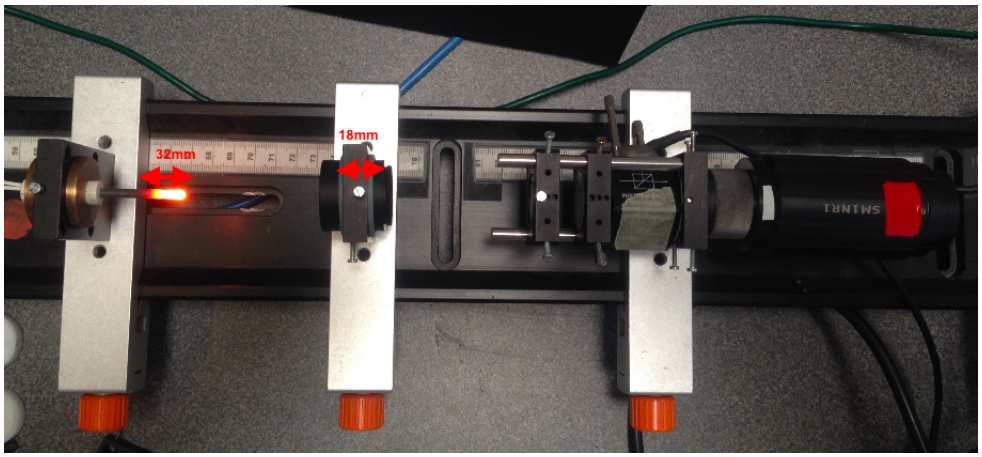

Figure 4.1: Configuration of the setup for the determination of the focal length of the lens

The way to obtain this distance consists in doing the following with one of the photodiodes (in this case photodiode 2 has been the chosen one). The voltage is measured for different distances of the lens from IR-emitter (sixteen different positions with steps of 1 mm) for three different positions of the photodiode (A, B and C). Then that distance of the lens where the voltage measured is practically the same in A, B and C is the wanted one. It is really important to take into account that the measurement of the distances is made in the optical rail scale and bewtween the brackets in order to be more

precise. So these two distances indicated in Fig.4.1 which show the distance between the first bracket and the tip of the emitter (32mm) and the distance between the second bracket and the flat surface of the lens (18mm) must be considered.

Taking into account the mentioned distances, the results are presented in Tab.4.1.

d (mm)	61	62	63	64	65	66	67	68
V_A **(V)**	9.21	9.51	9.68	10.00	10.29	10.60	10.88	11.03
V_B **(V)**	8.80	9.13	9.40	9.72	10.00	10.34	10.75	10.89
V_C **(V)**	9.00	9.44	9.76	10.02	10.33	10.69	11.03	11.04

d (mm)	69	70	71	72	73	74	75	76
V_A **(V)**	11.04	11.04	11.03	11.03	11.03	11.03	11.02	11.02
V_B **(V)**	11.04	11.04	11.03	11.03	11.03	11.03	11.02	11.02
V_C **(V)**	11.04	11.03	11.02	11.02	11.02	111.01	11.01	11.01

Table 4.1: Measured voltages by photodiode 2 in three different positions for different positions of the lens (where d is the distance between the tip of the emitter and the lens flat surface and V_A, V_B, V_C are the voltages measured for positions A, B and C)

Therefore analyzing Tab.4.1 the distance of the lens where the measured voltage by the photodiode in these three different positions is the same is 69mm. After this experiment this distance between the tip of the IR-emitter and the flat surface of the lens has not been changed.

Another way to calculate this focal length made in [28] consists in finding that position of the lens where the voltage measured by both photodiodes is the same. In fact this method has been used for a first approximation using the oscilloscope in order to know the range of distances to be analyzed. However this method could have some deviations related to the multiplier of the amplifier for each photodiode and the high sensitivity of each photodiode so with the applied method experiment is considered to have been improved.

4.2 Testing of the setup with the LabVIEW program and without it

Once the whole assembly is installed it has been tested using an oscilloscope, a signal generator and the matlab program (method 1) and also using the new LabVIEW program (method 2) with the aim of proving that the electro-optical device is able to measure the state of polarisation of a fully linear polarised infrared radiation. It has been performed with both methods to guarantee that the new LabVIEW program is working exactly as the other one and that the results are really similar. For it a pair of voltages is chosen ($V_1 = 0V$, $V_2 = 1V$ with the corresponding retardances 0,63 and 0,16 in this case) and 8 different positions of the polariser (position 1 is that where polariser and analyser and

aligned and then the next positions are the previous one plus 45°) in order to generate different polarisation angles. As consequence of the fact that linear polarisation states are symmetrical around the wave propagation axis, the polarisation range is completely defined between -90° and 90°, nevertheless the measurements have been carried out in the whole circumference in order to understand how the measurements are being carried out. The results of this test is presented in Tab.4.2 and it shows:

- Measured voltages with method 1: $\vec{V_{m1}} = \begin{pmatrix} V_{phot1full} \\ V_{phot2_V1} \\ V_{phot2_V2} \end{pmatrix}$
- Computed angle with method 1: ϕ_{c1}
- Computed Stokes vector with method 1: $\vec{S_{c1}} = \begin{pmatrix} S_{c0} \\ S_{c1} \\ S_{c2} \end{pmatrix}$.
- Measured voltages with method 2: $\vec{V_{m2}} = \begin{pmatrix} V_{phot1full} \\ V_{phot2_V1} \\ V_{phot2_V2} \end{pmatrix}$
- Computed angle with method 2: ϕ_{c2}
- Computed Stokes vector with method 2: $\vec{S_{c2}} = \begin{pmatrix} S_{c0} \\ S_{c1} \\ S_{c2} \end{pmatrix}$.

Position Num	**Measured voltages** $\vec{V_{m1}}$	**Computed Stokes vector** $\vec{S_{c1}}$	**Computed angle** ϕ_{c1}	**Measured voltages** $\vec{V_{m2}}$	**Computed Stokes vector** $\vec{S_{c2}}$	**Computed angle** ϕ_{c2}
1	$\begin{pmatrix} 6.10V \\ 2.90V \\ 3.54V \end{pmatrix}$	$\begin{pmatrix} 1 \\ 0.27 \\ -0.87 \end{pmatrix}$	37.27º	$\begin{pmatrix} 6.06V \\ 2.93V \\ 3.39V \end{pmatrix}$	$\begin{pmatrix} 1 \\ 0.19 \\ -0.06 \end{pmatrix}$	39,35º
2 (+45º)	$\begin{pmatrix} 6.15V \\ 3.50V \\ 3.34V \end{pmatrix}$	$\begin{pmatrix} 1 \\ 0.09 \\ 0.18 \end{pmatrix}$	42.47º	$\begin{pmatrix} 6.07V \\ 3.65V \\ 3.53V \end{pmatrix}$	$\begin{pmatrix} 1 \\ 0.17 \\ 0.24 \end{pmatrix}$	40.11º
3 (+90º)	$\begin{pmatrix} 6.20V \\ 1.56V \\ 1.08V \end{pmatrix}$	$\begin{pmatrix} 1 \\ -0.71 \\ -0.44 \end{pmatrix}$	67.42º	$\begin{pmatrix} 6.29V \\ 1.73V \\ 1.25V \end{pmatrix}$	$\begin{pmatrix} 1 \\ -0.65 \\ -0.39 \end{pmatrix}$	65.24º
4 (+135º)	$\begin{pmatrix} 6.17V \\ 1.02V \\ 1.15V \end{pmatrix}$	$\begin{pmatrix} 1 \\ -0.60 \\ -0.67 \end{pmatrix}$	63.54º	$\begin{pmatrix} 6.33V \\ 1.03V \\ 1.12V \end{pmatrix}$	$\begin{pmatrix} 1 \\ -0.59 \\ -0.68 \end{pmatrix}$	63.45º
5 (+180º)	$\begin{pmatrix} 6.20V \\ 2.98V \\ 3.45V \end{pmatrix}$	$\begin{pmatrix} 1 \\ 0.20 \\ -0.06 \end{pmatrix}$	39.38º	$\begin{pmatrix} 6.21V \\ 2.97V \\ 3.45V \end{pmatrix}$	$\begin{pmatrix} 1 \\ 0.18 \\ -0.08 \end{pmatrix}$	39,81º
6 (+225º)	$\begin{pmatrix} 6.40V \\ 3.57V \\ 3.35V \end{pmatrix}$	$\begin{pmatrix} 1 \\ 0.04 \\ 0.16 \end{pmatrix}$	43.82º	$\begin{pmatrix} 6.25V \\ 3.77V \\ 3.58V \end{pmatrix}$	$\begin{pmatrix} 1 \\ 0.16 \\ 0.23 \end{pmatrix}$	40.52º
7 (+270º)	$\begin{pmatrix} 6.55V \\ 1.71V \\ 1.22V \end{pmatrix}$	$\begin{pmatrix} 1 \\ -0.68 \\ -0.43 \end{pmatrix}$	66.36º	$\begin{pmatrix} 6.39V \\ 1.67V \\ 1.22V \end{pmatrix}$	$\begin{pmatrix} 1 \\ -0.66 \\ -0.42 \end{pmatrix}$	65.77º
8 (+315º)	$\begin{pmatrix} 6.48V \\ 1.13V \\ 1.38V \end{pmatrix}$	$\begin{pmatrix} 1 \\ -0.54 \\ -0.67 \end{pmatrix}$	61.18º	$\begin{pmatrix} 6.30V \\ 0.99V \\ 1.12V \end{pmatrix}$	$\begin{pmatrix} 1 \\ -0.62 \\ -0.64 \end{pmatrix}$	64.12º

Table 4.2: Derivation of various incident linear polarisation states for voltage pair (0V;2V), with LCVR phase shifts taken for 1550nm at 25º C

So observing this table many conclusions can be said. First of all and the most important is that both methods are not working correctly beause of the measured angle of polarisation and the Stokes vector have no sense and this is a really big problem in the objective of measuring the state of polarisation. Nevertheless this table is really interesting and then other conclusions can be drawn. The results obtained with both methods are really similar and moreover it is possible to observe that the results are also the same if the polariser is rotated 180º. Therefore this indicates that the LabVIEW program is working as it was expected, nevertheless both are getting wrong results so it is necessary to make a checking of the whole setup in order to find possible sources for erroneous measurements as it is shown in the next Sec.4.3.

4.3 Checking of the electro-optical device behavior

The aim of this section is to guarantee that the electro-optical device is working as it should do and for it many different experiments and conclusions are obtained. This section has been performed because the testing of the setup in order to measure the state of polarisation was not working correctly and therefore a cheking of the whole device was necessary to search possible causes for the problems.

First of all the possible misalignment of the assembly is checked and for it the following test has been carried out. It is performed because optical paths for each photodiodes are different. In this experiment the polariser, analyser and LCVR are not necessary, just the lens, filter and both photodiodes (also BS is necessary to take the measurements with photodiode 1) are used. For it different voltages and intensities of the thermal emitter has been applied and the voltages measured by photodiode 1 and photodiode 2 have been recorded as it is presented in Tab.4.3.

Measure Num	1	2	3	4
V_{phot1} **(V)**	11.3	11.2	11.1	6.6
V_{phot2} **(V)**	11.3	11.2	11.1	6.4
V and I IR-emitter (V)	12V 5.1A	10V 4.6A	8V 4.1A	6V 3.7A

Table 4.3: Voltages measured by photodiodes 1 and 2 for different conditions of the emitted light by the IR-emitter

So observing this table, different conclusions can be said because the measured values by both photodiodes are nearly exactly the same, with the exception of the last measurement but it is due to the fact that the emitted light is very low. Therefore first of all the lens are correctly positioned (the placing has been made with the precision of 1mm and as it can be seen in Sec. 4.1 the deviation produced by moving it 1 mm is considerable, nevertheless it could lead to small inaccuracies and not for the big mistake that is being searched) and components are aligned so the signals measured by both photodiodes do not depend on the optical path that they have followed. Also this means that both photodiodes are working correctly and the amplifier has the same multiplier in both outputs. This last fact could also be proved by exchanging photodiodes, changing photodiode 1 with photodiode 2 and vice versa.

Also in relation with a possible wrong behavior of cables these have been checked in the following way: by changing electrical connections to oscilloscope and also by changing electrical connections to the NI-PCI 6024E card. As consequence cables with both methods are checked.

Both polarisers must be checked and different aspects should be inspected. At first it has been checked if they are correctly mounted inside their housings and the conclusions are that one of them is perfectly placed while the other (the analyser) moves a

little bit what could lead to inaccuracies, nevertheless mounting it inside it housing and being careful when it is placed in the assembly it should work in a proper way. Secondly if the set of both polariser is working as it was expected is inspected. So for it the lens, filter, both polariser and photodiode 1 have been used (LCVR is not necessary). The test consists in checking if it is possible to see maximum output if both polarisers are parallel and minimum output if both polarisers are rotated by 90°.
In Fig.4.2 the configuration of both polarisers (Fig.4.2a) in parallel form and the measured voltage by photodiode 1 (Fig.4.2b) is shown.

(a) Placing of both polarisers in parallel form

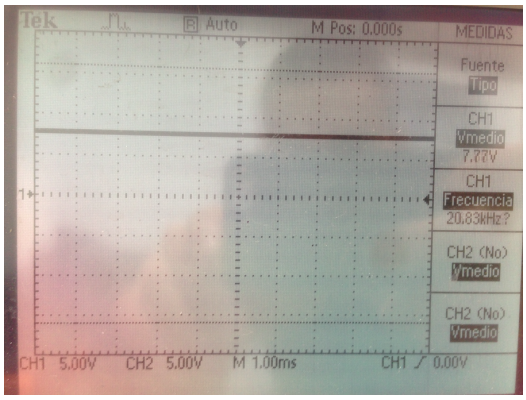

(b) Measured voltage by photodiode 1 shown in an oscilloscope

Figure 4.2: Test with polarisers in parallel position

In Fig.4.3 the configuration of both polarisers (Fig.4.3a) in perpendicular form and the measured voltage by photodiode 1 (Fig.4.3b) is shown.

(a) Placing of both polarisers in perpendicular form

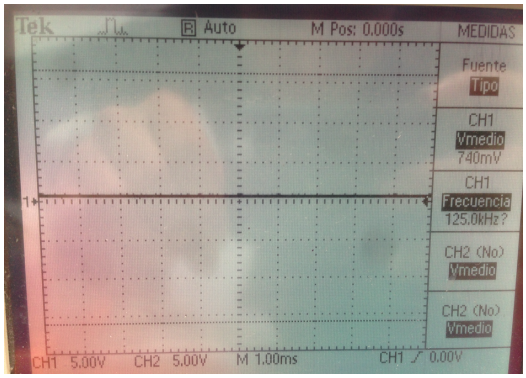

(b) Measured voltage by photodiode 1 shown in an osciloscope

Figure 4.3: Test with polarisers in perpendicular position

As it can be observed in Fig.4.2 and Fig.4.3, the set of both polarisers is working correctly because of for a parallel position the measured value is maximum which is 7.77V

and it they are perpendicular (one of them is rotated 90º) then the measured value is minimum which is nearly 0 and it is 0.73V. This is really important because in order to make the measurements to calculate the angle of polarisation it must work correctly to place correctly the polariser which is PSG component which allows the generation of that angle. For this positioning it is necessary to use this polariser and the analyser. The way to proceed is the following: at first all the components between polariser and analyser must be removed (filter should stay), then the analyser should be fixed aligned horizontally and finally the polariser is rotated while the intensity in the ouput of the analyser (photodiode 2) is being measured. An oscilloscope can be used to measure the intensity and both polarisers must be aligned when the measured voltage is maximum.

Thirdly it must be checked if the behavior of both polarisers is the same because these are exactly the same component and so the measurements obtained should be the same independently of the polariser that is being used. For it just the lens, filter, both polarisers and one photodiode has been used. Firstly one polariser is used in two different positions (rotation states) and measurements made by photodiode 1 are recorded and then the other polariser is used in these two same positions (rotation states) and the same is done. The obtained results are shown in Tab.4.4.

Position	1	2
V_{phot1} **(V) with polariser 1**	7.91	7.70
V_{phot1} **(V) with polariser 2**	7.85	7.72

Table 4.4: Voltages measured by photodiode 1 for two positions of polarisers

Also the CCM5-BS018/M non-polarising beam-splitter can have an inaccurated performance (a deviation around 10 % can be reached). To analyze if it is working correctly, different polarisation angles with the polariser has been generated (8 different positions) and it is observed if the intensity measured by photodiode 1 depends on this angle. It is shown in Tab.4.5 and each position is the previous plus 45º.

Position of polariser	1	2	3	4	5	6	7	8
Full intensity (in V)	6.10	6.15	6.20	6.17	6.20	6.40	6.55	6.48

Table 4.5: Influence of the incident polarisation angle on the non-polarising beam splitter behavior

Therefore observing Tab.4.5 that the non-polarising beam-splitter has a considerable influence on the outgoing full intensity (the two extrem values recorded are $6.10V$ and $6.55V$) so it can be one the main sources of inaccuracies of the setup and as it will be commented later in Sec.5.2 it would be a good idea to replace it.

Moreover the way to know which polarisation state is being generated by the polariser is not very precise, the gratuated circle shown in Fig.1.4 is used and as consequence this can lead to deviations. Another possible imprecision source could be the LCVR azi-

muthal angle positioning because it has been done in an approximate way, nevertheless as it is proved in [28] it does not have a really strong influence.

So the sum of all these possible causes can lead to small inaccuracies nevertheless it is considered that it still does not explain the results that are being obtained because of they totally have no sense. When a polarisation angle is being generated by the PSG and the next is the previous one plus 45°, the computed angles should be coherent and measure the first one and the second is the previous plus 45°, nontheless this is not happening.

5 Recommendations for further studies

The aim of this section consists in suggesting how this investigation should be continued and for it some improvements for the LabVIEW program and for the setup are proposed. These suggestions are also focused on finding possible sources for erroneous measurements with the goal of making possible the reproduction of the experiments about measuring the state of polarisation of the infrared light emitted by the thermal emittter.

After that experiment the investigation should continue with the positioning of the electro-optical device onto a robot for laser welding so regarding it a really good explanation with schemes, how to perform the computation and pictures is given in [28], so to make this last step it can be consulted. However it must be commented that for this final goal the PSG which is generating a fully linear polarised polarisation state should be removed, because in that case the heated workpiece would be the one which would generate a partially linear polarised infrared radiation. The used setup should be able to measure this partially linear polarised light which it would consists just in the PSA, without thermal emitter or polariser. So finally it would be possible the computation of polarisation state and with it the inclination angle.

5.1 Enhancements to the LabVIEW program

The presented program already has a good performance, nevertheless it can be improved in the following way in order to make the process faster. The sampling time in the current program is one second per step so it could be decreased much more. A proposed way to make this reduction consists in decreasing this sampling time slowly and making tests of accuracy and repeatability and choose that sampling time where these tests are acceptable. In this way if the sampling time is reduced to 100ms the process would be ten times faster and because of the final goal is to install it for industrial processes it could suppose many advantages. However the fulfilment of this new improvement would change the structure that should be used for the program. Now the program should be carried out as a sequence where this sampling time can be arranged as it is desired for each test. It would be very similar, just the structure should be changed and then the block diagram in each frame would be practically the same as the one which has been used. To overcome this goal using a Timed Sequence structure is suggested. A Timed Sequence structure consists of one or more frames, timed by an internal or external timing source that execute sequentially.

Moreover if it would be required that the three steps should be executed more than one time as a Timed Sequence structure executes each frame only once then this struc-

ture could be replaced by a Timed Loop. Nevertheless these are just suggestions and other ways to get the same result can be performed.

Another point that should be improved is the function that approximates the behavior of the LCVR which relates retardance and applied RMS voltage. This improvement must be done because of the existing function which is a polynomial one of degree six approximates correctly between 1V and 8V. So it should be found another way to get a proper function which fits better with the behavior of the LCVR. One way could be the following: have three different approximation functions, one for each range (0,1-1V, 1V-8V and 8V-10V) and then in the block diagram conditional blocks should be used and depending on the introduced voltage the program should use one function or other to compute the retardance. So between 1V and 8V (if voltage is equal to 1V or higher and less than 8V) the current computed function would be used, between 0,1 and 1V (if voltage is equal to 0,1V or higher and less than 1V) another polynomial function of degree six could be a good option (Fig.5.1a) and between 8V and 10V (if voltage is equal to 8V or higher and equal to 10V or less) a potential function could be a proper choice (Fig.5.1b).

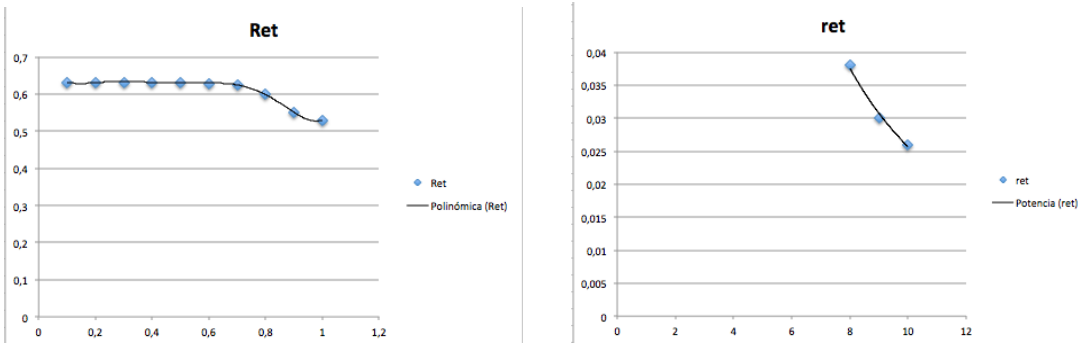

(a) Polynomial approximation function between 0,1V and 1V

(b) Potential approximation funtion between 8V and 10V

Figure 5.1: Suggested approximation functions for the LCVR behavior

5.2 Enhancements to the setup

First of all the source of erroneous measurements should be found and for it some more actions can be done.

As it has already been said before the analyser is not really well fixed in its housing and as consequence if it is not set carefully it moves inside the housing and then the behavior is not the required one. Also if the electro-optical device is manipulated to add or remove other components the rest of the assembly is slightly moved so this analyser could not stay in the right position. It could be solved by using another housing which would hold it in a proper way.

Regarding the LCVR it could be more deeply checked in the following way. A voltage lower than 1V must be applied to the LCVR what would mean that it is working as a half wave plate and as consequence it should rotate the incoming linear polarised light by 2alpha. Then two different situations must be analyzed. The first situation consists in placing both polarisers (polariser and analyser) perpendicularly and with the LCVR orientated at 45° between them. So the LCVR should rotate the incoming horizontally polarised incoming light by 90° and as consequence it would pass through the analyser in the same direction as the analyser one and must give a maximum output. The second situation consists in performing the same test, however in this case polarisers should be set parallel and then the obtained output should be minimum (almost zero) because when it passes through the LCVR it is rotated 90° and then perpendicular to the analyser direction of polarisation. If both situations happen then the LCVR should be working correctly.

Assuming that the source of errors is found some improvements can be done in the setup. One simple solution to possible deviations due to misalignment of the components could be using four shafts instead of two that are being used now. Nevertheless this solution is not that easy for technical reasons related to adapters and housings. Moreover the CCM5-BS018/M non-polarising beam splitter should be replaced by a more precise component because the deviation that it can introduce in the measurements is really considerable and therefore a suggestion is made in [28] about using a Polka Dot Beam splitter [21].

The reproduction of the experiments to determinate the state of polarisation would consist in the following measurements. For each polarisation state measurement two voltages (applied to the LCVR) are necessary. Then the phase shift introduced by the LCVR for these voltages would be automatically computed by the LabVIEW program with the approximation function. The results of both tests could be shown with these following parameters:

- Introduced polarisation angle: ϕ_i
- Computed polarisation angle: ϕ_c
- Angular deviation: $\delta_{phi} = |\phi_i - \phi_c|$
- Introduced Stokes vector (theoretically calculated): $\vec{S_a} = \begin{pmatrix} S_{i0} \\ S_{i1} \\ S_{i2} \end{pmatrix}$
- Computed Stokes vector: $\vec{S_c} = \begin{pmatrix} S_{c0} \\ S_{c1} \\ S_{c2} \end{pmatrix}$
- Root-mean-square deviation [37]: $\delta_{RMSD} = \sqrt{\frac{(S_{i0}-S_{c0})^2+(S_{i1}-S_{c1})^2+(S_{i2}-S_{c2})^2}{3}}$.

It would only be necessary to introduce angles between -90° and 90° because the whole polarisation range is completely defined between them. Finally these angular and root-mean square deviations could be analyzed in order to get conlcusions about how precise or imprecise the measurements and computation have been done.

5.3 Possible alternatives

If finally the source of erroneous measurements is not found and as consequence the experiment of determining the state of polarisation can not be performed, then some alternatives are suggested.

A new setup could be built using the same components, however changing the CM5-BS018/M non-polarising beam splitter by the Polka Dot Beam splitter and also fixing correctly the analyser in its housing. The lens could be removed and then to solve the problem of the beam divergence influence the following could be done. Optical paths of both photodiodes are currently different so without lens the effect of divergence would be really important, therefore to avoid this influence one solution could be that optical paths of photodiode 1 and 2 have the same length. To achieve these goal different adapters would be necessary and also it would be really interesting to reduce the size of the whole assembly in order to make it more compact.

6 Conclusions

In this Bachelor's Thesis an existing setup for measuring the state of polarisation of an infrared radiation has been improved, focusing on the electronics of the system.

At first all the components have been analyzed and assembled in order to reproduce the assembly made in [28]. Secondly the setup has been improved by unifying different tasks in one LabVIEW program with the aim of having a more compact system which is fully automated. These different tasks consists in the monitoring of LCVR, the realization of the measurements and the computation of the polarisation state which before were made using different devices and programs. Thirdly the electro-optical device has been tested with the new LabVIEW program and without it (performing the experiment as it was done before) in order to compute the azimuthal angle of polarisation and the Stokes vector of a fully linear polarised light emitted by a thermal emitter, nevertheless using both methods the results have not been as it was expected. As these results are really similar using both methods it is considered that the LabVIEW program works correctly, then possible sources for erroneous measurements have been examined. As consequence many different aspects of the device have been checked and some possible causes for small inaccuracies have been found nevertheless it has not been detected which is the real problem that makes getting wrong measurements.

Moreover some recommendations have been suggested to make the LabVIEW program faster and also more precise. For it another way to put together all the parts of the program with a Timed Sequence structure is explained and how to get different approximation functions to obtain the retardance introduced by the LCVR depending on the applied voltage is commented. As well some possible ways to improve the setup are described and also which results should be given if the setup works correctly and possible alternatives if it does not work are commented.

The final goal of this assembly consists in computing the state of polarisation and with it the inclined angle of the keyhole in order to make an online monitoring and adaptive control during a real laser processes, specifically it would be transfered onto a robot for laser welding. However due to the problems that have been faced it is a pending task for next investigations that will continue with the development of this electro-optical device.

List of Figures

List of Tables

References

[1] Optech consulting. Access date: 15/03/2017. URL: http://www.optech-consulting.com/html/laser_market_data.html.

[2] National Instruments. Access date: 08/05/2017. URL: http://www.ni.com/pdf/manuals/370719c.pdf.

[3] National Instruments. Access date: 10/05/2017. URL: http://www.ni.com/pdf/manuals/373987a.pdf.

[4] National Instruments. Access date: 13/04/2017. URL: http://www.ni.com/pdf/manuals/371303n.pdf.

[5] Ionix. Access date: 18/03/2017. URL: http://www.ionix.fi/en/technologies/laser-processing/laser-welding/.

[6] The University of Texas at Arlington. Access date: 12/05/2017. URL: http://www.uta.edu/optics/research/ellipsometry/ellipsometry.htm.

[7] Electrical4u. Access date: 12/05/2017. URL: https://www.electrical4u.com/black-body-radiation/.

[8] Molecular expressions. Access date: 28/03/2017. URL: https://micro.magnet.fsu.edu/primer/java/electromagnetic/.

[9] Phelafel. Access date: 18/04/2017. URL: http://phelafel.technion.ac.il/~hilag/tutorial/LCPhases.html.

[10] Thorlabs. Access date: 14/04/2017. URL: https://www.thorlabs.com/newgrouppage9.cfm?objectgroup_id=6179.

[11] Hawkeye Technologies. Access date: 23/04/2017. URL: IR-Si295,%20Hawk%20Eye%20Techn%E2%80%A6.

[12] Thorlabs. Access date: 16/04/2017. URL: https://www.thorlabs.com/drawings/6bb605527c9cd65d-179E5726-9AA3-FC45-7F7049A672A4F16D/LA4306-AutoCADPDF.pdf.

[13] Thorlabs. Access date: 16/04/2017. URL: https://www.thorlabs.de/images/TabImages/PBS_1200_G2-780.gif.

[14] Interferenzoptik bk. Access date: 16/04/2017. URL: http://www.interferenzoptik.de/1080nm-1880nm_en.htm.

[15] Thorlabs. Access date: 17/04/2017. URL: https://www.thorlabs.de/images/TabImages/LCC1xx1-C_Transmission_780.gif.

[16] Thorlabs. Access date: 17/04/2017. URL: https://www.thorlabs.de/newgrouppage9.cfm?objectgroup_id=6179.

[17] Thorlabs. Access date: 16/04/2017. URL: https://www.thorlabs.de/images/large/TTN040010-lrg.jpg.

[18] Hamamatsu. Access date: 18/04/2017. URL: https://www.hamamatsu.com/blobs/1328779674576?blobheadername1=content-disposition&blobheadervalue1=inline%3Bfilename%3Dk_g8370-01_-81_pp_xx.jpg&ssbinary=true.

[19] Hamamatsu. Access date: 18/04/2017. URL: https://www.hamamatsu.com/us/en/product/alpha/P/4107/G12180-010A/index.html.

[20] Thorlabs. Access date: 17/04/2017. URL: https://www.thorlabs.de/newgrouppage9.cfm?objectgroup_id=6179.

[21] Thorlabs. Access date: 30/05/2017. URL: https://www.thorlabs.com/newgrouppage9.cfm?objectgroup_id=1110&gclid=CjwKEAjwsLTJBRCvibaW9bGLtUESJAC4wKw1dHVDpIFMyNKAxci_yJvRpmw3J-1A5_u4fHWUHATYChoCQGnw_wcB.

[22] Access date: 15/05/2017. URL: http://www.ni.com/pdf/products/us/4daqsc202-204_ETC_212-213.pdf.

[23] *Advances in Laser Materials Processing*. Elsevier Science & Technology, 27th July 2010. 848 pp. ISBN: 1845694740. URL: http://www.ebook.de/de/product/19472540/advances_in_laser_materials_processing.html.

[24] Susan L. Blakeney, Sally E. Day and J. Neil Stewart. 'Determination of unknown input polarisation using a twisted nematic liquid crystal display with fixed components'. In: *Optics Communications* 214.1–6 (2002), pp. 1–8. ISSN: 0030-4018. DOI: http://dx.doi.org/10.1016/S0030-4018(02)02115-6. URL: http://www.sciencedirect.com/science/article/pii/S0030401802021156.

[25] Juan M Bueno. 'Polarimetry using liquid-crystal variable retarders: theory and calibration'. In: *Journal of Optics A: Pure and Applied Optics* 2.3 (2000), p. 216. URL: http://stacks.iop.org/1464-4258/2/i=3/a=308.

[26] D. Clarke and J.F. Grainger. *Polarized light and optical measurement*. International series of monographs in natural philosophy. Pergamon Press, 1971. URL: https://books.google.ie/books?id=agUvAAAAIAAJ.

[27] Todorka L. Dimitrova and Antoine Weis. 'A double demonstration experiment for the dual nature of light'. In: ed. by Peter A. Atanasov et al. SPIE, Mar. 2007. DOI: 10.1117/12.726898.

[28] Pierre Drobniak. 'Measurement of the state of polarisation of partially linear polarised infrared radiation by means of nematic liquid crystals'. MA thesis. 2016.

[29] W. W. Duley. *Laser Welding*. JOHN WILEY & SONS INC, 11th Oct. 1998. 264 pp. ISBN: 0471246794. URL: http://www.ebook.de/de/product/3606358/w_w_duley_laser_welding.html.

[30] S. Chandrasekhar F.R.S. *Liquid Crystals*. Cambridge University Press, 2010. ISBN: 9780511622496. URL: https://www.amazon.com/Liquid-Crystals-S-Chandrasekhar-F-R-S/dp/051162249X?SubscriptionId=0JYN1NVW651KCA56C102&tag=techkie-20&linkCode=xm2&camp=2025&creative=165953&creativeASIN=051162249X.

[31] Hongping Gu and W W Duley. 'A statistical approach to acoustic monitoring of laser welding'. In: *Journal of Physics D: Applied Physics* 29.3 (Mar. 1996), pp. 556–560. DOI: 10.1088/0022-3727/29/3/011.

[32] E. Hecht. *Optik*. Addison-Wesley, 1989. ISBN: 9783925118869. URL: https://books.google.at/books?id=lzCnSgAACAAJ.

[33] John Ion. *Laser Processing of Engineering Materials: Principles, Procedure and Industrial Application*. Butterworth-Heinemann, 2005. ISBN: 978-0-7506-6079-2. URL: https://www.amazon.com/Laser-Processing-Engineering-Materials-Application-ebook/dp/B001075RAA?SubscriptionId=0JYN1NVW651KCA56C102&tag=techkie-20&linkCode=xm2&camp=2025&creative=165953&creativeASIN=B001075RAA.

[34] Claes Johnson. 'Mathematical Physics of BlackBody Radiation'. In: (). URL: http://www.csc.kth.se/~cgjoh/ambsblack.pdf.

[35] I.C. Khoo. *Liquid Crystals*. Wiley Series in Pure and Applied Optics. Wiley, 2007. ISBN: 9780471751533. URL: https://books.google.at/books?id=o0tRAAAAMAAJ.

[36] David S Kliger and James W Lewis. *Polarized light in optics and spectroscopy*. Elsevier, 2012.

[37] Kazuhiko Kobayashi and Moin Us Salam. 'Comparing simulated and measured values using mean squared deviation and its components'. In: *Agronomy Journal* 92.2 (2000), pp. 345–352.

[38] Fanrong Kong and Radovan Kovacevic. 'Development of a Comprehensive Process Model for Hybrid Laser-Arc Welding'. In: *Welding Processes*. InTech, Nov. 2012. DOI: 10.5772/45850.

[39] L Li, D J Brookfield and W M Steen. 'Plasma charge sensor for in-process, non-contact monitoring of the laser welding process'. In: *Measurement Science and Technology* 7.4 (Apr. 1996), pp. 615–626. DOI: 10.1088/0957-0233/7/4/019.

[40] Akira Matsunawa et al. 'Dynamics of keyhole and molten pool in laser welding'. In: *Journal of Laser Applications* 10.6 (Dec. 1998), pp. 247–254. DOI: 10.2351/1.521858.

[41] Thomas Pauger. 'Diodenbasierte Prozessüberwachung eines Remote-Schneidprozesses basierend auf einer Polarisationsmessung'. MA thesis. Adolf-Blamauer-Gasse 1-3 / Rella-Halle 1030 Wien: TUWien, Institut für Fertigungstechnik und Hochleistungslasertechnik, 2014.

[42] G. S. Ranganath. 'Black-body radiation'. In: *Resonance* 13.2 (Feb. 2008), pp. 115–133. DOI: 10.1007/s12045-008-0028-7.

[43] Peter Schaaf, ed. *Laser Processing of Materials*. Springer Berlin Heidelberg, 2010. DOI: 10.1007/978-3-642-13281-0.

[44] Kailash K. Sharma. *Optics: Principles and Applications*. Academic Press, 2006. ISBN: 0-12-370611-4. URL: https://www.amazon.com/Optics-Principles-Applications-Kailash-Sharma/dp/0123706114?SubscriptionId=0JYN1NVW651KCA56C102&tag=techkie-20&linkCode=xm2&camp=2025&creative=165953&creativeASIN=0123706114.

[45] Shri Singh. *Liquid Crystals: Fundamentals*. WORLD SCIENTIFIC PUB CO INC, 11th Nov. 2002. 548 pp. ISBN: 9810242506. URL: http://www.ebook.de/de/product/3804858/shri_singh_liquid_crystals_fundamentals.html.

[46] Jan Weberpals et al. 'Utilisation of Thermal Radiation for Process Monitoring'. In: *Physics Procedia* 12 (2011), pp. 704–711. DOI: 10.1016/j.phpro.2011.03.088.

[47] Wladyslaw A. Wozniak, Marzena Pretka and Piotr Kurzynowski. 'Imaging Stokes polarimeter based on a single liquid crystal variable retarder'. In: *Appl. Opt.* 54.20 (July 2015). DOI: 10.1364/AO.54.006177. URL: http://ao.osa.org/abstract.cfm?URI=ao-54-20-6177.

7 Appendix

7.1 Technical data of the PCI NI-6024E card

In Tab.7.1 a summary about the main technical data of the card PCI NI-6024E is given.

PCI NI 6024E features

Main features	
Bus	PCI, PCMCIA
Analog Inputs	16 SE/8 DI
Input Resolution	12 bits
Max. Sampling Rate	200 kS/s
Input Range	± 0,05 to ± 10 V
Analog Outputs	2
Output Resolution	12 bits
Output Rate	10 kS/s
Output Range	± 10 V
Digital I/O	8
Counter/Timers	2, 24-bit
Triggers	Digital

Table 7.1: Technical data NI PCI 6024E card [22]

7.2 Lens dimensions

These are the dimensions of the lens which are shown in Fig.7.1 and are really important in order to know the diameter of the parallel light beam.

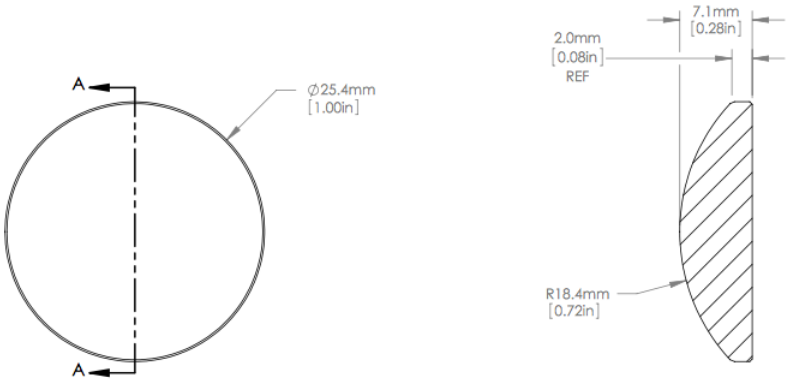

Figure 7.1: LA4306 lens dimensions (Thorlabs datasheet) [12]

7.3 Splitting behavior of the CCM1-PBS254/M beam-splitter

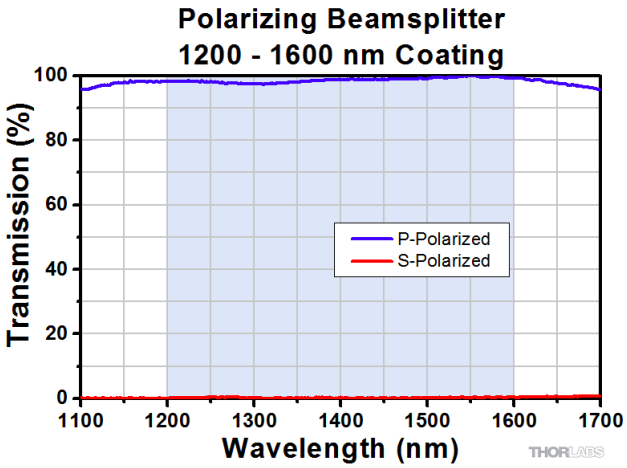

Figure 7.2: Splitting behavior of one output of the CCMM1-PBS254/M beam splitter [13]

7.4 Filtering behavior of the bk-1500-090-B bandpass filter

Here it is a representation in Fig.7.3 of the relation between the transmission coefficient of the bk-1500-090-B bandpass filter and wavelength.

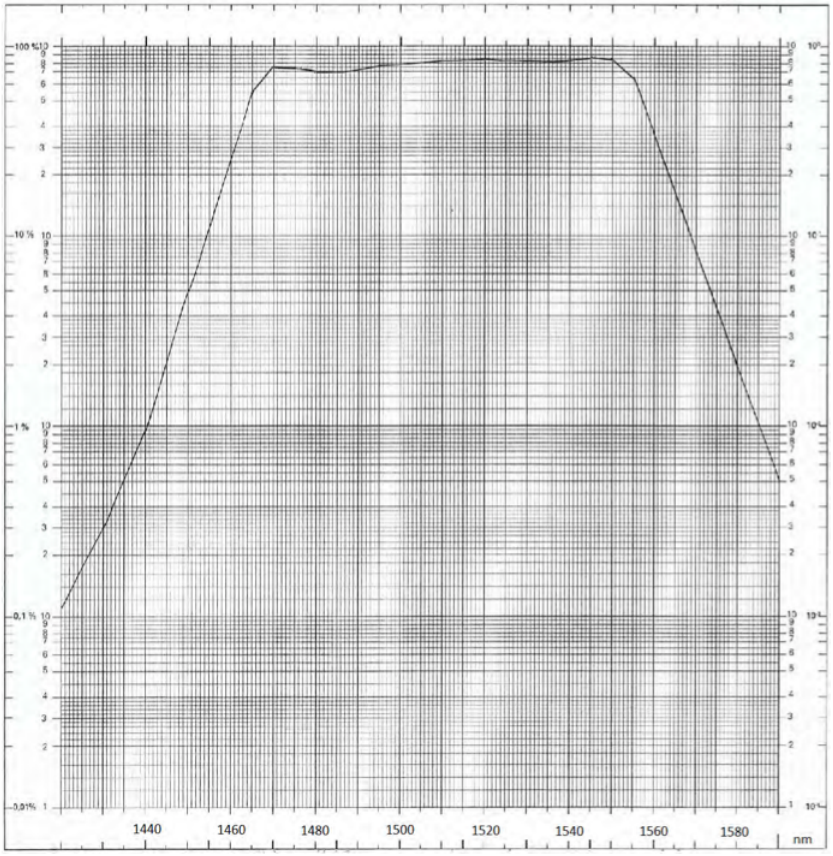

Figure 7.3: Filtering behavior of the bk-1500-090-B bandpass filter [28]

7.5 Transmission coefficient of the LCVR

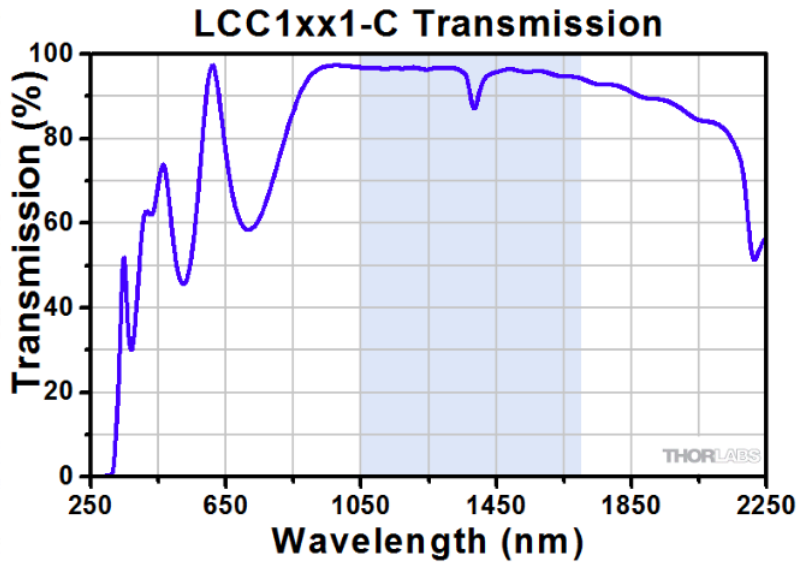

Figure 7.4: Transmission coeffiecient of the LCC1111-C LCVR depending on the wavelength [15]